A PROGRAMMING APPROACH TO THE SOLUTION OF PROBLEMS INVOLVING ELASTIC-PLASTIC PLATES

by

G.P. Mitchell

A thesis submitted in partial fulfillment of the requirements for the degree of Master of Science (Engineering)

Department of Civil Engineering
University of Cape Town

September 1982

DECLARATION OF CANDIDATE

I hereby declare that this thesis is my own work and that it has not been submitted for a degree at any other university

Signed by candidate

G.P. Mitchell.

ACKNOWLEGEMENTS

I wish to express my thanks to the following:

Dr B D Reddy who suggested the topic and supervised the research;

Professor J B Martin for helpful discussions;

Mrs V Atkinson and Mrs P Jordaan who typed this thesis;

the C.S.I.R. for financial support;

Mr H Cable for printing this thesis.

ABSTRACT

An extended kinematic minimum principle in classical plasticity is used as the basis for the finite element formulation of the rate problem for elastic-plastic plates. A simple algorithm is used to solve the resulting quadratic programming problem. The numerical solution of the problem is carried out in two ways: one method involves load step sizes which are scaled so that one or more gauss points just become plastic, and the other method involves load step sizes which are fixed once and for all at the outset. Examples are given and discussed.

CONTENTS

DECLARATION		(i)
ACKNOWLEDGEMENTS		(ii)
ABSTRACT		(iii)
CONTENTS		(iv)
NOTATION AND LIST OF SYMBOLS		(vi)
CHAPTER 1	INTRODUCTION	1
CHAPTER 2	THE BASIC EQUATIONS AND THE EXTENDED KINEMATIC MINIMUM PRINCIPLE FOR THE RATE PROBLEM	4
2.1	Introduction	4
2.2	Basic Equations	4
2.3	The Classical Rate Problem in Elasto-Plasticity	8
2.4	The Extended Kinematic Minimum Principle	10
CHAPTER 3	FINITE ELEMENT PLATE ANALYSIS	13
3.1	Introduction	13
3.2	Plate Bending Elements	13
3.3	The Heterosis Element	16
3.4	Elastic-Plastic Plate Analysis	24
CHAPTER 4	FORMULATION OF PRESENT APPROACH	26
4.1	Introduction	26
4.2	Mindlin Plate Equations	26
4.3	Finite Element Discretisation	28
4.4	An Algorithm for the Minimisation of $\bar{U}_p^o$	35
4.5	Incremental Solution Procedure	37

CHAPTER 5	ELASTIC-PLASTIC STATE DETERMINATION SCHEMES	39
5.1	Introduction	39
5.2	General Equations	40
5.3	Elastic Predictor-Radial Corrector Method	45
5.4	Tangent Predictor-Radial Return Method	48
CHAPTER 6	NUMERICAL IMPLEMENTATION	50
6.1	Introduction	50
6.2	Formation of $\overset{*}{\underset{\approx}{K}}$ and the Solution of $\overset{*}{\underset{\approx}{K}}(\Delta\underset{\sim}{d} \,\vdots\, \lambda') = (\Delta\underset{\sim}{P} \,\vdots\, \underset{\sim}{0})$	51
6.3	Procedures for Incremental Solution Involving a Scaled Load Vector	53
6.4	Implementation of the Elastic-Plastic State Determination Schemes	56
6.5	Program Description	59
CHAPTER 7	NUMERICAL EXAMPLES	62
7.1	Introduction	62
7.2	Circular Plate	62
7.3	Square Plate	69
7.4	Cyclic Loading	75
7.5	Circular Plate with Central Hole	77
7.6	Cruciform Plate	80
CHAPTER 8	CONCLUSIONS	82
	REFERENCES	84

NOTATION AND LIST OF SYMBOLS

A	-	initial yield value in yield function
$\underset{\approx}{B}$	-	deformation matrix
C_{ijkl}	-	elastic constitutive tensor
D_{ijkl}	-	inverse of elastic constitutive tensor
$\underset{\sim}{d}$	-	vector of nodal degrees of freedom
E	-	Young's modulus
E_p	-	plastic modulus
E_T	-	tangent modulus
$\underset{\sim}{e}$	-	deviatoric strain vector (plane stress components)
$\dot{e}$	-	effective shear strain rate
F	-	body forces
G	-	shear modulus
$\det J$	-	determinant of Jacobian matrix
$\underset{\approx}{K}$	-	stiffness matrix
k	-	loading history term in yield function
$\underset{\sim}{P}$	-	load vector
S	-	surface of a body
s	-	effective shear stress
$\underset{\sim}{s}$	-	deviatoric stress vector (plane stress components)
T	-	surface tractions
u,v,w	-	displacement variables in cartesian coordinate system x,y,z
V	-	volume of a body
W_p	-	plastic work
α	-	numerical integration constant

β - gradient of yield function

γ - engineering shear strain

ε - strain

θ - rotational variables defined in cartesian coordinate system

λ - plastic multiplier

ν - poisson's ratio

σ - stress

ϕ - yield function

Unless stated to the contrary the following convention for superscripts and subscripts applies:

e - pertaining to an element/or the elastic part

p - the plastic part

T - transpose of a vector or matrix

Subscripts

Tensor notation with the normal summation convention is used and subscripts i through s are reserved for components of tensors.

e - pertaining to an element

f - flexural contribution

pqr - may refer to a particular numerical integration point; then summation convention does not apply

s - shear contribution

$\Delta( )$ - denotes an increment in the quantity in brackets

$\dot{( )}$ - denotes the rate of the quantity in brackets

$( )'$ - indicates some weighted value of the quantity in brackets

$\sim$ - denotes a vector

$\approx$ - denotes a matrix

CHAPTER 1

INTRODUCTION

By comparison with problems involving elastic materials, few analytical solutions are available for elastic-plastic solids and recourse has generally to be made to numerical methods in order to obtain approximate results. The minimum principles governing the mechanical behaviour of elastic-plastic solids were first introduced by Hodge and Prager (1948) and Greenberg (1949), and these are normally used in conjunction with the finite element method, which discretises the continuum spatial field into a finite number of parameters.

Direct methods of exploiting these minimum principles for incremental elasto-plasticity problems and using the finite element method include the initial stress (Zienkiewicz, Valliapan and King (1969)) and the tangent modulus (Marcal and King (1967)) approaches. The system stiffness matrix for the former method is inverted once only and equilibrium iterations are necessary for a converged solution as the plastic strain increments of subsequent load increments become larger. For the tangent modulus approach the system matrix is inverted at each incremental step. Some iterations will generally still be required, but obviously much less than for the initial stress approach. The tangent modulus approach has been used extensively and is implemented in most major elastic-plastic finite element packages.

An alternative to the direct methods has been to formulate the elastic-plastic problem as a formal mathematical programming

problem and to use programming techniques in the solution (Sayegh and Rubenstein (1972)). Elastic-plastic finite element analyses using this approach have been used by De Donato and Franchi (1977). In order to formulate the programming problem in the incremental manner the yield surface is assumed to be piecewise linear. An optimisation technique is also used to enable large continuum problems with small plastic zones to be analysed. Not much information is available on the computational efficiency of these methods (Cottle (1977)). Although there is ongoing research in this area the author has not found any subsequent papers on this subject in the available literature.

Maier (1969) has presented a kinematic minimum principle which results in a quadratic programming problem. In an attempt to derive Maier's result from the classical kinematic principle Martin (1975) has established an extended kinematic minimum principle for the rate problem in elasto-plasticity which involves a continuous functional subject to inequality constraints. Instead of resorting to quadratic programming techniques for its solution Martin and Reddy (1977) have presented a simple algorithm in the context of truss problems which makes the numerical solution of the minimum principle straightforward. Dittmer (1978) has subsequently extended this approach to include plane stress/strain and axisymmetric problems.

In this study we take the extended minimum principle of Martin and apply it to plates subjected to transverse loading. Classical plasticity with a von Mises yield surface with isotropic hardening is used. Plasticity is allowed to spread through the thickness of the plate. For the finite element discretisation the recently developed

'heterosis' plate bending element is used. In addition, an improved solution scheme is employed which provides for an extremely efficient solution when compared with other numerical approaches to the problem.

The plan of this thesis is as follows: First we will introduce the constitutive equations for an elastic-plastic body and state the extended kinematic minimum principle for the rate problem. Next a brief review of the development of plate bending elements used in the finite element method is undertaken. The formulation of the 'heterosis' element is given and the inclusion of plastic behaviour in the element is discussed. In Chapter 4 the finite element discretisation of the functional used in the minimum principle is presented together with the minimisation algorithm. We next discuss the numerical procedures necessary for the implementation of the incremental problem and the resulting set of equations. A brief review of the elastic-plastic state determination schemes used to give a more efficient solution is also given. Finally, in Chapter 7, we present a few selected examples and compare with other numerical or analytical solutions where possible.

CHAPTER 2

THE BASIC EQUATIONS AND THE KINEMATIC MINIMUM PRINCIPLE FOR THE RATE PROBLEM

2.1 Introduction

Consider a body of volume V with a surface S in a cartesian coordinate system x_i. The body is subjected to body forces $F_i(x_k)$ on V, surface tractions $T_i(x_k)$ on part of the surface S_T and prescribed displacements $u_i(x_k)$ on the remainder of the surface S_U. Displacements are assumed to be small and loading is quasi-static. We limit our discussion to isotropic homogeneous elastic-plastic materials. For the plastic behaviour we use a von Mises yield criterion with isotropic hardening.

In the following section the governing relations which comprise the equilibrium, kinematic and constitutive equations, are given. Thereafter, we formulate the rate problem for an elastic-plastic body and discuss kinematic minimum principles.

2.2 Basic Equations

The equilibrium equations are

$$\frac{\partial \sigma_{ij}}{\partial x_j} + F_i = 0 \quad \text{on } V \quad , \tag{2.1}$$

$$\sigma_{ij} = \sigma_{ji} \quad , \tag{2.2}$$

and

$$\sigma_{ij} \nu_j = T_i \quad \text{on } S_T \quad , \tag{2.3}$$

where σ_{ij} is the stress tensor and ν_j the outward normal from the surface. A statically admissable set of forces, tractions and stresses must satisfy equations (2.1), (2.2) and (2.3).

The strain tensor is given by the strain-displacement relations

$$\varepsilon_{ij} = \frac{1}{2}\left(\frac{\partial u_i}{\partial x_j} + \frac{\partial u_j}{\partial x_i}\right) \quad . \tag{2.4}$$

A kinematically admissable set of strains and displacements must satisfy equation (2.4) and the compatibility condition

$$\frac{\partial^2 \varepsilon_{ij}}{\partial x_k \partial x_\ell} + \frac{\partial^2 \varepsilon_{k\ell}}{\partial x_i \partial x_j} = \frac{\partial^2 \varepsilon_{ij}}{\partial x_j \partial x_\ell} + \frac{\partial^2 \varepsilon_{k\ell}}{\partial x_i \partial x_k} \quad . \tag{2.5}$$

We divide the total strain into an elastic and plastic part, i.e.

$$\varepsilon_{ij} = \varepsilon^e_{ij} + \varepsilon^p_{ij} \quad . \tag{2.6}$$

The elastic strain and stress are related by

$$\varepsilon^e_{ij} = C_{ijk\ell}\sigma_{k\ell} \quad , \tag{2.7}$$

where $C_{ijk\ell}$ is an isotropic fourth order tensor.

To describe the plastic behaviour we introduce a continuously differentiable convex yield function ϕ. It may be written as a function of the stress and a plastic work term which is a measure of the amount of permanent deformation which has occurred, i.e. $\phi = \phi(\sigma_{ij}, W_p)$. For $\phi < 0$ there is no change in plastic strains. When $\phi = 0$ and $\frac{\partial \phi}{\partial \sigma_{ij}} \, d\sigma_{ij} < 0$, unloading occurs and we again have no change in plastic strain. Only if $\phi = 0$ $\frac{\partial \phi}{\partial \sigma_{ij}} \, d\sigma_{ij} \geq 0$, i.e. when loading

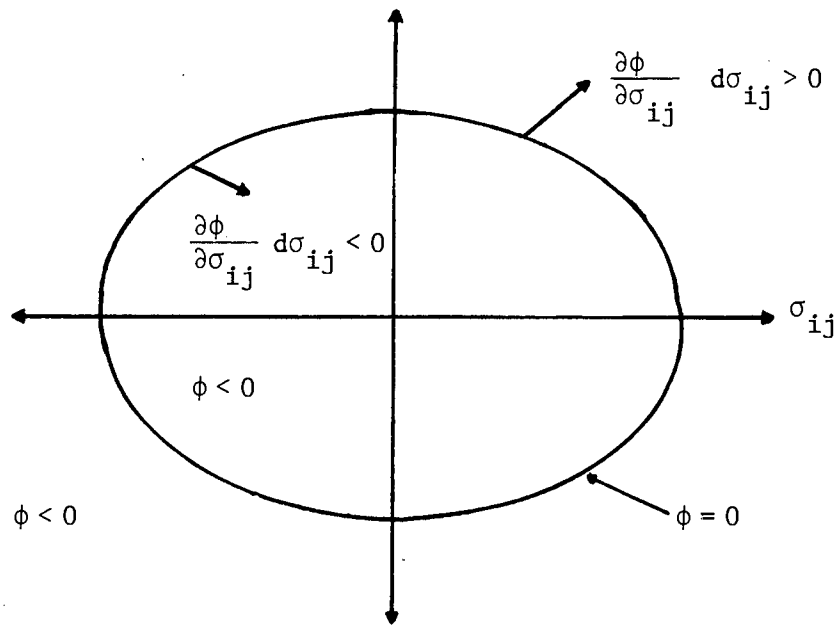

Figure 2.1 Stress Increments in Stress Space.

occurs, do we obtain any plastic strain increments. States of stress such that $\phi > 0$ are not allowed. The plastic strain increments that do occur are proportional to the gradient of the yield function.

We can thus write

$$d\varepsilon^p_{ij} = 0 \quad \text{if} \quad \phi < 0$$

$$\text{or} \quad \phi = 0 \quad \text{and} \quad \frac{\partial \phi}{\partial \sigma_{ij}} < 0 \tag{2.8}$$

and

$$d\varepsilon^p_{ij} = \lambda \frac{\partial \phi}{\partial \sigma_{ij}} \quad \text{if } \phi = 0 \text{ and } \frac{\partial \phi}{\partial \sigma_{ij}} d\sigma_{ij} \geq 0 \tag{2.9}$$

where λ is some non-negative scalar.

For an elastic plastic material we have

$$\lambda = G(\sigma_{ij}, W_p) \frac{\partial \phi}{\partial \sigma_{k\ell}} d\sigma_{k\ell} \tag{2.10}$$

with $G \geq 0$ (see Martin (1978)).

We obtain the elastic-perfectly plastic case if we let $G \to \infty$. This implies, from equation (2.10), that $\frac{\partial \phi}{\partial \sigma_{k\ell}} d\sigma_{k\ell} = 0$ for λ to be finite. Note that for loading $\dot{\phi} = 0$ and

$$\frac{\partial \phi}{\partial \sigma_{ij}} d\sigma_{ij} + \frac{\partial \phi}{\partial W_p} dW_p = 0 \tag{2.11}$$

so that, for the perfectly plastic case, $dW_p = 0$ we can write $\phi = \phi(\sigma_{ij})$.

The von Mises yield criterion assumes that plastic deformation occurs when the shear stress on the octahedral plane reaches a certain value. The yield function then has the form

$$\phi = s - k^{\frac{1}{2}} \tag{2.12}$$

where

$$s = \{\frac{1}{3}[\sigma_{ij}\,\sigma_{ij} - \frac{1}{3}(\sigma_{kk})^2]\}^{\frac{1}{2}} \quad ,$$

$$k = A + c\,W_p \quad ,$$

$$W_p = \int \sigma_{ij}\, d\varepsilon^p_{ij} \quad .$$

Here, A defines the initial yield value and c is some constant. Note that s has the same form as the second invariant of the stress deviator tensor.

Following Dittmer (1978) we introduce

$$1/G = c/2\, \frac{\partial\phi}{\partial\sigma_{k\ell}}\, \frac{\partial\phi}{\partial\sigma_{k\ell}} \tag{2.13}$$

for the case of simple tension we then obtain

$$c/2 = E_p = E\,E_T/(E - E_T) \tag{2.14}$$

E_p is the plastic modulus, E_T the tangent modulus and E the Young's modulus for the material.

2.3 The Classical Rate Problem in Elasto-Plasticity

The classical rate problem in elasto-plasticity may be stated as follows (Martin and Reddy (1977)). Consider a body of volume V and surface S. Surface tractions $T_i(x_k,\tau)$ are prescribed on part of the

surface S_T, displacements $u_i(x_k,\tau)$ are prescribed on the remainder of the surface S_U, and body forces $F_i(x_k,\tau)$ on V are prescribed over the interval $0 \leq \tau \leq t$. We wish to determine the reactions $T_i(x_k,\tau)$ on S_U, the displacements $u_i(x_k,\tau)$ on S_T and V, and the stress field $\sigma_{ij}(x_k,\tau)$ and strain field $\varepsilon_{ij}(x_k,\tau)$ in V for $0 \leq \tau \leq t$.

The rate problem at time t may be considered to be preceded by a succession of rate problems over the time interval $0 \leq \tau \leq t$. Assuming that the complete solution at time t is known, we now consider body force rates $\dot{F}_i$ on V, surface traction rates $\dot{T}_i$ on S_T and displacement rates $\dot{u}_i$ on S_U. We are then required to find the reaction rates $\dot{T}_i$ on S_U, displacement rates $\dot{u}_i$ on S_T and V, and the stress rate field $\dot{\sigma}_{ij}$ and strain rate field $\dot{\varepsilon}_{ij}$ in V. Equations (2.1) - (2.10) are easily rewritten in rate form, i.e.

$$\frac{\partial \dot{\sigma}_{ij}}{\partial x_j} + \dot{F}_i = 0 \qquad \text{on V} \tag{2.15}$$

$$\dot{\sigma}_{ij}\, \nu_j = \dot{T}_i \qquad \text{on S} \tag{2.16}$$

$$\dot{\varepsilon}_{ij} = \frac{1}{2}\left(\frac{\partial \dot{u}_i}{\partial x_j} + \frac{\partial \dot{u}_j}{\partial x_i} \right) \text{ on V} \tag{2.17}$$

$$\dot{\varepsilon}_{ij} = \dot{\varepsilon}^e_{ij} + \dot{\varepsilon}^p_{ij} \tag{2.18}$$

$$\dot{\varepsilon}^e_{ij} = C_{ijk\ell}\, \dot{\sigma}_{k\ell} \tag{2.19}$$

$$\dot{\varepsilon}^p_{ij} = 0 \quad \text{if} \quad \phi < 0 \quad \text{or} \quad \phi = 0 \text{ and } \frac{\partial \phi}{\partial \sigma_{ij}}\, \dot{\sigma}_{ij} < 0 \tag{2.20}$$

$$\dot{\varepsilon}^p_{ij} = \frac{\partial \phi}{\partial \sigma_{ij}} \quad \text{if } \phi = 0 \text{ and } \frac{\partial \phi}{\partial \sigma_{ij}}\, \dot{\sigma}_{ij} \geq 0 \tag{2.21}$$

Equation (2.19) may be inverted, to obtain

$$\dot{\sigma}_{ij} = D_{ijk\ell}\, \dot{\varepsilon}^{e}_{k} \tag{2.22}$$

where $D_{ijk\ell}$ is the inverse of $C_{ijk\ell}$.

The inverted constitutive equations are (Martin (1975))

$$\dot{\sigma}_{ij} = D_{ijk\ell}\, \dot{\varepsilon}_{k\ell} \quad \text{for } \phi < 0$$

$$\text{or } \phi = 0 \text{ and } D_{ijk\ell} \frac{\partial \phi}{\partial \sigma_{ij}} \dot{\varepsilon}_{k\ell} \leq 0$$

$$\dot{\sigma}_{ij} = D_{ijk\ell}\, \dot{\varepsilon}_{k\ell} - D_{ijk\ell} \frac{\partial \phi}{\partial \sigma_{k\ell}} \left[\frac{D_{pqrs} \frac{\partial \phi}{\partial_{pq}} \dot{\varepsilon}_{rs}}{1/G + D_{mnhg} \frac{\partial \phi}{\partial \sigma_{mn}} \frac{\partial \phi}{\partial \sigma_{hg}}} \right]$$

$$\text{for } \phi = 0 \quad \text{and} \quad D_{ijk\ell} \frac{\partial \phi}{\partial \sigma_{ij}} \dot{\varepsilon}_{k\ell} \geq 0 \tag{2.23}$$

The elastic, perfectly plastic case is obtained when $G \to \infty$.

2.4 The Extended Kinematic Minimum Principle

The classical minimum principles for the elastic-plastic rate problem have been in existence for some time (Hodge and Prager (1948) and Greenberg (1949)). Consider the potential function $W^{o} = W^{o}(\dot{\varepsilon}_{ij})$, where

$$\dot{\sigma}_{ij} = \frac{\partial W^{o}}{\partial \dot{\varepsilon}_{ij}} \quad ; \tag{2.24}$$

here,

$$W^{o} = \frac{1}{2} D_{ijk\ell}\, \dot{\varepsilon}_{ij}\, \dot{\varepsilon}_{k\ell} \quad \text{for } \phi < 0$$

$$\text{or} \quad = 0 \quad \text{and} \quad D_{ijk\ell} \frac{\partial \phi}{\partial \sigma_{ij}} \dot{\varepsilon}_{k\ell} \leq 0$$

and

$$W^{o} = \frac{1}{2} D_{ijk\ell} \dot{\varepsilon}_{ij} \dot{\varepsilon}_{k\ell} - \frac{1}{2} \frac{(D_{ijk\ell} \frac{\partial \phi}{\partial \sigma_{ij}} \dot{\varepsilon}_{k\ell})^2}{(1/G + D_{pqrs} \frac{\partial \phi}{\partial \sigma_{pq}} \frac{\partial \phi}{\partial \sigma_{rs}})}$$

$$\text{for } \phi = 0 \quad \text{and} \quad D_{ijk\ell} \frac{\partial \phi}{\partial \sigma_{ij}} \dot{\varepsilon}_{k\ell} \geq 0$$

Suppose that $\dot{\varepsilon}^{*}_{ij}$, $\dot{u}^{*}_{i}$ defined on V satisfy equation (2.17) and the kinematic boundary conditions $\dot{u}^{*}_{i} = \dot{u}_{i}$ on S_U; then we can construct a kinematic minimum principle for the rate problem. The solution $\dot{\varepsilon}_{ij}$, $\dot{u}_{i}$ to the rate problem is that member of the class $\dot{\varepsilon}^{*}_{ij}$, $\dot{u}^{*}_{i}$ which renders an absolute minimum the functional

$$U^{o}_{p}(\dot{\varepsilon}^{*}_{ij}, \dot{u}^{*}_{i}) = \int_{V} W^{o}(\dot{\varepsilon}^{*}_{ij}) \, dV - \int_{V} \dot{F}_{i} \dot{u}^{*}_{i} \, dV - \int_{V} \dot{T}_{i} \dot{u}^{*}_{i} \, dS \qquad (2.25)$$

Difficulties can arise in the solution of (2.25) as the derivatives of W^{o} are discontinuous.

Martin (1975) has extended the minimum principle (2.25) by replacing W^{o} by a continuously differentiable function subject to inequality constraints. The body is now divided into two regions. The elastic part said to be in V_e and the plastic part in V_p. A non-negative scalar field $\lambda^{*}(x_i)$ is introduced over V_p. Martin introduces the function

$$\bar{W}^{o}(\dot{\varepsilon}^{*}_{ij}, \lambda^{*}) = \frac{1}{2} D_{ijk\ell} (\dot{\varepsilon}^{*}_{ij} - \lambda^{*} \frac{\partial \phi}{\partial \sigma_{ij}})(\dot{\varepsilon}^{*}_{k\ell} - \lambda^{*} \frac{\partial \phi}{\partial \sigma_{k\ell}}) + \frac{\lambda^{*}}{2G} \qquad (2.26)$$

and the constraints

$$\lambda^{*} = 0 \quad \text{in } V_e, \qquad \phi < 0$$

$$\lambda^{*} \geq 0 \quad \text{in } V_p, \qquad \phi = 0 \quad ,$$

and shows that the solution of the rate problem is given by that member of the class $\dot{\varepsilon}^{*}_{ij}$, λ^{*}, $\dot{u}^{*}_{i}$ which renders an absolute minimum the functional

$$\bar{U}^{o}_{p}(\dot{\varepsilon}^{*}_{ij}, \lambda^{*}, \dot{u}^{*}_{i}) = \int_{V} \bar{W}^{o}(\dot{\varepsilon}^{*}_{ij}, \lambda^{*}) dV - \int_{V} \dot{F}_{i}\, \dot{u}^{*}_{i}\, dV - \int_{S_T} \dot{T}_{i}\, \dot{u}^{*}_{i}\, dS \qquad (2.27)$$

subject to the constraints

$$\lambda^{*} = 0 \quad \text{in } V_{e}, \qquad \phi < 0$$

$$\lambda^{*} \geq 0 \quad \text{in } V_{p}, \qquad \phi = 0$$

CHAPTER 3

FINITE ELEMENT PLATE ANALYSIS

3.1 Introduction

As stated earlier the finite element method will be used in conjunction with the extended minimum principle presented in Chapter 2, to solve the rate problem. The form of the functional for discretised plates is relatively straightforward to obtain and will be discussed in Chapter 4.

The choice of a plate finite element dictates to a large extent the accuracy of the solution. For many years researchers have been trying to develop an accurate and reliable plate bending element. From these developments have come several plate and shell elements which may be considered feasible; some of them are discussed in the next section. Of these, the heterosis element of Hughes and Cohen (1978) seems the most readily programmable and free of most of the problems associated with plate bending elements, and is accordingly chosen for this study. We will also discuss how elastic-plastic material behaviour is implemented in the element.

3.2 Plate Bending Elements

Initial approaches in the finite element analysis of plates used the classical Kirchoff theory as a starting point for the formulation of the problem. These models were either based on the generalised displacement method, hybrid or mixed formulations. A good review of

earlier work has been undertaken by Gallagher (1969). Although some elements were accurate, because of the higher order polynomials used and the requirement of continuity of displacements across the element boundaries, the formulations tended to be complicated. In addition, the specification of boundary conditions was difficult as it involved nodal derivative degrees of freedom of order greater than one. In attempts to simplify these models the accuracy or reliability invariably declined.

With the introduction of isoparametric elements researchers moved away from the classical plate theory in the development of new elements. Recent successful elements are the hybrid stress plate element of Spilker and Munir (1980), the stress plate element of Robinson (1977), the moderately thick shell element of McNeal (1978), the semi-Loof shell element of Irons (1978) and the general shell element of Bathe (1980). All of these formulations accommodate transverse shear stresses in one way or another. A common method, first used by Oden and Wempner (1969) and applied to the semi-Loof element, is to constrain the shear strain terms to zero at a number of discrete points in the element; this is known as the discrete Kirchhoff hypothesis. Although the formulation is rather complicated it has been implemented successfully and applied to a number of non-linear problems (see Martins and Owen (1981) and Javaherian, Dowling and Lyons (1980)). However, for a non-linear analysis in which the stiffness matrix is reconstituted at least at every incremental step, a simpler formulation is desirable.

The isoparametric elements based on the plate theory of Mindlin (1951) and

in which the transverse displacement and rotations are interpolated independently, have become increasingly popular. These elements use either the 8-noded Serendipity or one of the Lagrange family of interpolation functions. Provision is made for constant shear strains through the thickness. The strain energy is then decomposed into flexural and shear contributions. Although these elements perform well for moderately thick plates, they become over-stiff as the aspect ratio increases, due to the shear terms dominating, and they tend to 'lock', i.e. as the thickness of the plate is reduced, we effectively introduce constraints that the shear is zero. This leads, in some cases, to an overconstrained element. Malkus and Hughes (1978) introduced the constraint index, a heuristic measure of the ability of the element to accommodate these implied constraints. To alleviate this problem Hughes, Taylor and Kanoknukulchai (1977) and Pugh, Hinton and Zienkiewicz (1978) used reduced integration schemes to under-integrate the stiffness matrix. Improved results were obtained, but spurious zero energy modes were now introduced into the stiffness matrix. Although most of these spurious modes are constrained when these elements are used in a mesh, the user is never certain when they may 'act up' or not. Most of these spurious zero energy modes are eliminated if a selective reduced integration scheme is used, i.e. in which only the shear terms are under-integrated. A good review of these techniques with examples is given by Hughes, Cohen and Haroun (1978).

From their investigations Hughes and Cohen (1978) have introduced the 'Heterosis' element in which the transverse displacement is interpolated by the 8 - noded Serendipity shape functions and the rota-

tions by the 9 - noded Lagrange shape functions. This element is accurate for moderately thick and for most thin plate applications. It contains no spurious zero energy modes and has a favourable constraint index.

A recent paper by Hughes and Tezduyar (1981) explores anew the concepts involved in Mindlin plate elements and present a new four-node bilinear isoparametric element.

3.3 The Heterosis Element

The original formulation for the heterosis element is given by Hughes and Cohen (1978). An elastic-plastic plate analysis using the element is presented by Hinton and Owen (1981). Hinton and Owen use the Serendipty shape functions for all the boundary node degrees of freedom and only introduce the Lagrange shape function for the central node. However for this study, the separate shape functions for the rotations and displacements are used and for completeness we present the formulation as implemented.

We consider the plate to lie in the x - y plane with the normal tractions on the upper and lower free surfaces, Fig. 3.1. The basic assumptions of Mindlin plate bending theory are:

1. Only small displacements are considered.
2. Straight lines through the thickness remain straight and do not extend.
3. Normals to the mid-surface do not necessarily remain normal.
4. The plate is in a state of approximate plane stress.

The displacements in the x, y and z directions are then, respectively,

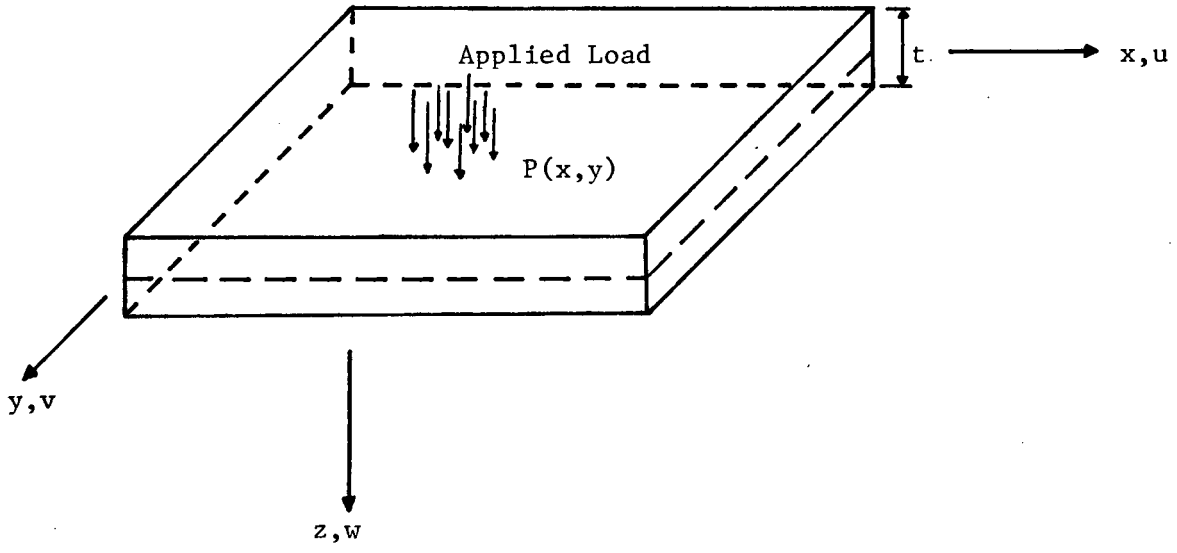

Figure 3.1 Orientation of Plate in Cartesian Coordinate System

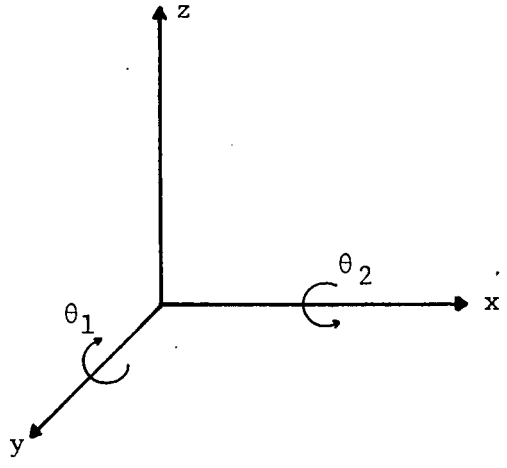

Figure 3.2 θ_1 and θ_2 Rotations.

$$
\begin{aligned}
u(x,y,z) &= - z\theta_1 \ (x,y) \quad , \\
v(x,y,z) &= - z\theta_2 \ (x,y) \quad , \\
w(x,y,z) &= w(x,y) \quad ,
\end{aligned}
\tag{3.1}
$$

where

$$
\begin{Bmatrix} \theta_1 \\ \theta_2 \end{Bmatrix} = \begin{bmatrix} 0 & -1 \\ 1 & 0 \end{bmatrix} \begin{Bmatrix} \theta_x \\ \theta_y \end{Bmatrix} \quad ;
$$

θ_x, θ_y are the rotations about lines parallel to the x- and y-axes, respectively, according to the right hand screw rule. The strain-displacement relations are then

$$
\varepsilon_x = \frac{\partial u}{\partial x} = - z \frac{\partial \theta_1}{\partial x}
$$

$$
\varepsilon_y = \frac{\partial v}{\partial y} = - z \frac{\partial \theta_2}{\partial y}
$$

$$
\gamma_{xy} = \left(\frac{\partial u}{\partial y} + \frac{\partial v}{\partial x} \right) = - z \left(\frac{\partial \theta_1}{\partial y} + \frac{\partial \theta_2}{\partial x} \right) \tag{3.2}
$$

$$
\gamma_{xy} = \frac{\partial w}{\partial x} - \theta_1
$$

$$
\gamma_{yz} = \frac{\partial w}{\partial y} - \theta_2
$$

where ε_x and ε_y are axial strains and γ_{xy}, γ_{xz}, γ_{yz} are engineering shear strains. We form a column vector of strains and partition into in-plane and out-of-plane terms:

$$
\underset{\sim}{\varepsilon} = \{ \varepsilon_x, \ \varepsilon_y, \ \gamma_{xy} \ \vdots \ \gamma_{xz}, \ \gamma_{yz} \}^T \quad . \tag{3.3}
$$

Also, we write

$$z\underset{\sim}{\varepsilon}_f = \left\{ -\frac{\partial\theta_1}{\partial x} \;,\; -\frac{\partial\theta_2}{\partial y} \;,\; -\left(\frac{\partial\theta_1}{\partial} + \frac{\partial\theta_2}{\partial x}\right) \right\}^T \;, \tag{3.4}$$

and

$$\underset{\sim}{\varepsilon}_s = \left\{ \left(\frac{\partial w}{\partial x} - \theta_1\right) \;,\; \left(\frac{\partial w}{\partial y} - \theta_2\right) \right\}^T \;. \tag{3.5}$$

The conventional form of the elastic strain energy for an isotropic elastic plate may now be written as

$$\frac{1}{2}\int_v \left(z^2 \underset{\sim}{\varepsilon}_f^T \underset{\approx}{D}_f \underset{\sim}{\varepsilon}_f + \underset{\sim}{\varepsilon}_s^T \underset{\approx}{D}_s \underset{\sim}{\varepsilon}_s \right) \tag{3.6}$$

with

$$\underset{\approx}{D}_f = \begin{bmatrix} 2\mu + \bar{\lambda} & \bar{\lambda} & 0 \\ & 2\mu + \bar{\lambda} & 0 \\ \text{sym} & & \mu \end{bmatrix}$$

and

$$\underset{\approx}{D}_s = \kappa\mu \begin{bmatrix} 1 & 0 \\ 0 & 1 \end{bmatrix}$$

where $\bar{\lambda} = 2\lambda\mu/(\lambda+2\mu)$, λ and μ are the Lame constants, and κ is a shear correction factor taken as 5/6.

The heterosis element is based on the conventional isoparametric formulation (Fig. 3.3). The natural coordinates ξ, η of the parent element vary from -1 to +1. It has 9 nodes with 26 degrees of freedom, i.e. two rotations and the transverse displacement at the 8 boundary nodes and two rotations at the centre node. The field variables $\underset{\sim}{u}^e = \{w^e, \theta_1^e, \theta_2^e\}^T$ and the nodal degrees of freedom

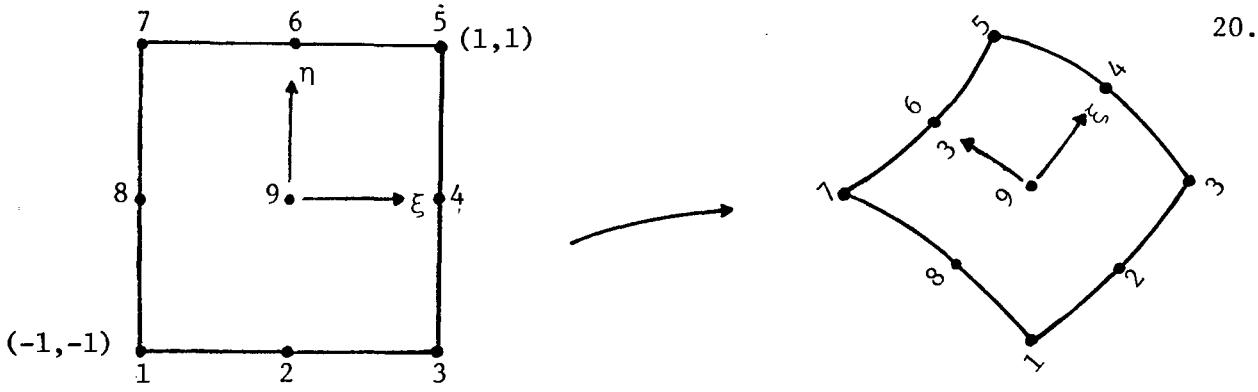

Figure 3.3 Heterosis Element.

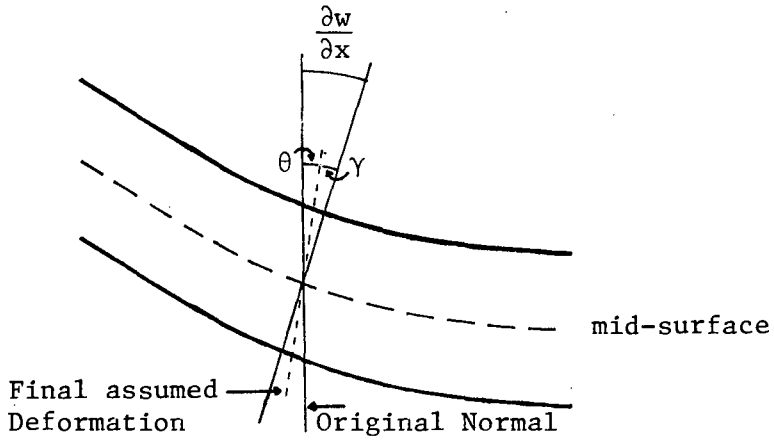

Figure 3.4 Assumed Deformation for Mindlin Theory.

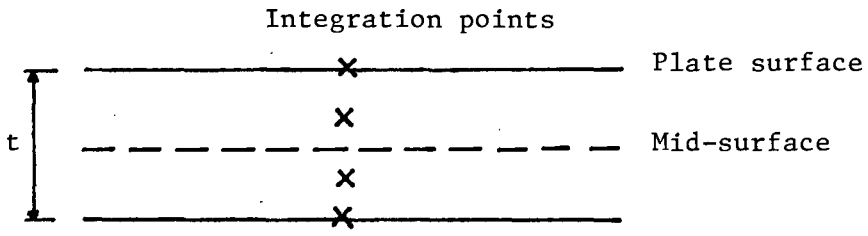

Figure 3.5 Schematic Representation of Integration through the Thickness of the Plate for 4 - point Rule.

$\underset{\sim}{d}_i^e = \{w_i^e, \theta_{1i}^e, \theta_{2i}^e\}^T$ defined at the mid-surface of the plate for element e in an assemblage are related by

$$\underset{\sim}{u}^e = \sum_{i=1}^{9} \underset{\approx}{N}_i \underset{\sim}{d}_i^e \tag{3.7}$$

where

$$\underset{\approx}{N}_i = \begin{bmatrix} S_i & 0 & 0 \\ 0 & L_i & 0 \\ 0 & 0 & L_i \end{bmatrix} \qquad \text{for} \quad i = 1,8$$

$$\underset{\approx}{N}_9 = \begin{bmatrix} L_9 & 0 \\ 0 & L_9 \end{bmatrix}$$

and S_i and L_i are the Serendipity and Lagrange shape functions, respectively, given in terms of the local coordinates ξ and η.

The Serendipity shape functions are:

- for corner nodes

$$S_i = \frac{1}{4}(1+\xi\xi_i)(1+\eta\eta_i)(\xi\xi_i+\eta\eta_i-1) \quad i = 1, 3, 5, 7 \quad ;$$

- for midside nodes (3.8)

$$S_i = \frac{\xi_i^2}{2}(1+\xi\xi_i)(1-\eta^2) + \frac{\eta_i^2}{2}(1+\eta\eta_i)(1-\xi^2) \quad i = 2, 4, 6, 8 \quad .$$

The Lagrange shape functions are:

- for corner nodes

$$L_i = \frac{1}{4}(\xi^2+\xi\xi_i)(\eta^2+\eta\eta_i) \quad i = 1, 3, 5, 7 \quad ;$$

- for midside nodes

$$L_i = \frac{1}{2}\xi_i^2(\xi-\xi\xi_i)(1-\xi^2) + \frac{1}{2}\xi_i^2(\xi-\xi\xi_i)(1-\xi^2) \quad i = 2, 4, 6, 8 \quad ;$$

- for the central node (3.9)

$$L_9 = (1-\xi^2)(1-\eta^2) \quad .$$

The element strains can now be written as

$$\underset{\sim}{\varepsilon}_f^e = \sum_{i=1}^{9} \underset{\approx}{B}_{fi} \underset{\sim}{d}_i^e \quad ,$$

$$\underset{\sim}{\varepsilon}_s^e = \sum_{i=1}^{9} \underset{\approx}{B}_{si} \underset{\sim}{d}_i^e \quad , \tag{3.10}$$

where

$$\underset{\approx}{B}_{fi} = \begin{bmatrix} 0 & -L_{i,x} & 0 \\ 0 & 0 & -L_{i,x} \\ 0 & -L_{i,x} & -L_{i,x} \end{bmatrix} \quad \text{for} \quad i = 1,8 \quad ,$$

$$\underset{\approx}{B}_{f9} = \begin{bmatrix} -L_{9,x} & 0 \\ 0 & -L_{9,y} \\ -L_{9,y} & -L_{9,x} \end{bmatrix} \quad ,$$

$$\underset{\approx}{B}_{si} = \begin{bmatrix} S_{i,x} & -L_i & 0 \\ S_{i,y} & 0 & -L_i \end{bmatrix} \quad \text{for} \quad i = 1,8 \quad ,$$

$$\underset{\approx}{B}_{s9} = \begin{bmatrix} -L_9 & 0 \\ 0 & -L_9 \end{bmatrix}$$

Note that a comma followed by a subscript in the above expressions denotes partial differentiation. The consistent load vector is calculated in the normal manner. As a result of the 3 and 2 degrees of freedom associated with the boundary nodes and at the centre node of the element, respectively, care must be taken to ensure that the correct

variables are associated with each other in the assembly of both the elastic stiffness matrix and the load vector.

To avoid any confusion in the geometric definition of the element we choose the coordinates of the centre node to be located at the origin of the natural coordinates of the Serendipity shape functions. Thus

$$x_9^e = \sum_{i=1}^{8} S_i(0,0)\, x_i^e \quad ,$$
$$y_9^e = \sum_{i=1}^{8} S_i(0,0)\, y_i^e \quad . \tag{3.11}$$

In the calculation of the Jacobian matrix to define the mapping of the element, only the Serendipity shape functions are used.

The elastic stiffness matrix obtained from equation (3.6) may be written as

$$\underset{\approx}{K}^e = \underset{\approx}{K}_f^e + \underset{\approx}{K}_s^e \tag{3.12}$$

where

$$\underset{\approx}{K}_f^e = \int_{V_e} \underset{\approx}{B}_f^T \underset{\approx}{D}_f \underset{\approx}{B}_f \, dV_e \quad ,$$

$$\underset{\approx}{K}_s^e = \int_{V_e} \underset{\approx}{B}_s^T \underset{\approx}{D}_s \underset{\approx}{B}_s \, dV_e \quad ,$$

$$\underset{\approx}{B}_f = [\underset{\approx}{B}_{f1}, \underset{\approx}{B}_{f2} \cdots\cdots \underset{\approx}{B}_{f9}] \quad ,$$

$$\underset{\approx}{B}_s = [\underset{\approx}{B}_{s1}, \underset{\approx}{B}_{s2} \cdots\cdots \underset{\approx}{B}_{s9}] \quad .$$

The flexural contribution is integrated using a 3 x 3 gaussian quadrature scheme and the shear term by a 2 x 2 scheme.

3.4 Elastic-Plastic Plate Analysis

Analytical solutions for elastic-plastic plates are mainly restricted to the calculation of limit loads of circular perfectly-plastic plates. In their book on plastic analysis and design Massonet and Save (1972) discuss some of the experimental work done and give the limit loads for circular plates. Extensive load/deflection graphs for various plates are also presented. Upper and lower bounds for the limit loads of rectangular plates are discussed by Hodge and Belytschko (1968), while other earlier work has been done by Popov et al (1967) and by Ang and Lopez (1968). Among more recent attempts using finite element techniques, the most noteworthy contributions are those by Barnard and Shaw (1976), Bathe and Bolourchi (1980), Javaherian, Dowling and Lyons (1980). Most of this work is based on the tangent modulus approach; stress resultants are used which implies that a plate section is considered to go plastic instantaneously. Both Tresca and von Mises yield conditions are implemented and hardening is allowed for.

In order to include the plastic behaviour of a plate in the Heterosis element certain assumptions are made in the present study. First, only flexural terms are contained in the yield conditions. This requirement is due to the selective reduced integration procedure used to evaluate the stiffness matrix. As all stresses should be evaluated at the gauss points (Barlow (1976)), the flexural and shear stresses are thus calculated at different locations within the element. According to Hinton and Owen (1980) this will not cause too great an error, provided the aspect ratio does not exceed a certain value. True stresses, instead of stress resultants will be calculated to allow

for the plasticity to spread through the depth of the plate. This will be done by evaluating the stresses at Newton-Cotes integration points through the thickness.

CHAPTER 4

FORMULATION OF PRESENT APPROACH

4.1 Introduction

The first stage in utilising the finite element method in conjunction with the extended minimum principle is the discretisation of the plate into appropriate elements. The formulation proceeds at element level and the global problem is obtained through a straightforward summation procedure. First we present the Mindlin plate equivalent of the equations in Chapter 2. Next we will show how a modified form of the conventional tangent stiffness matrix is derived. The extended minimum principle can then be written in matrix form. In the last section a simple algorithm for the solution of the resulting quadratic programming problem is given.

4.2 Mindlin Plate Equations

The Mindlin plate equations follow directly the assumptions in Chapter 3. The non-zero components of stress are the in-plane components σ_x, σ_y, σ_{xy} and the out-of-plane components τ_{xz}, τ_{yz}. The corresponding strains are ε_x, ε_y, γ_{xy}, γ_{xz} and γ_{yz}. The remaining components of stress and strain are either assumed zero or ignored in the analysis. This leads to a minor violation of the compatibility equation (2.5), although the error involved is negligible.

From Fig. 3.1, u, v and w are the displacements in the x, y and z directions, respectively. The rotations θ_1 and θ_2 are defined in equation (3.1). Thus we can relate equations (2.4) and (3.2), and we write

$$\varepsilon_{11} \equiv \varepsilon_x = \frac{\partial u}{\partial x} = - z \frac{\partial \theta_1}{\partial x} \quad ,$$

$$\varepsilon_{22} \equiv \varepsilon_y = \frac{\partial v}{\partial x} = - z \frac{\partial \theta_2}{\partial x} \quad ,$$

$$2\varepsilon_{12} \equiv \gamma_{xy} = \left(\frac{\partial u}{\partial y} + \frac{\partial v}{\partial x}\right) = - z \left(\frac{\partial \theta_1}{\partial y} + \frac{\partial \theta_2}{\partial x}\right) \quad , \tag{4.1}$$

$$2\varepsilon_{13} \equiv \gamma_{xz} = \frac{\partial w}{\partial x} - \theta_1 \quad ,$$

$$2\varepsilon_{23} \equiv \gamma_{yz} = \frac{\partial w}{\partial y} - \theta_2 \quad .$$

The constitutive equations (2.7) now become

$$\varepsilon_x^e = 1/E \, (\sigma_x - \nu\sigma_y) \quad ,$$

$$\varepsilon_y^e = 1/E \, (\sigma_y - \nu\sigma_z) \quad ,$$

$$\gamma_{xy}^e = 1/G \, \sigma_{xy} \quad ,$$

$$\gamma_{xz}^e = 1/G \, \tau_{xz} \quad ,$$

$$\gamma_{yz}^e = 1/G \, \tau_{yz} \quad .$$

where E is the elastic modulus, ν the Poisson's ratio and $G = E/2(1 + \nu)$ the shear modulus. We introduce stress and strain vectors, $\underset{\sim}{\sigma} = (\sigma_x, \sigma_y, \sigma_{xy}, \tau_{xz}, \tau_{yz})^T$ and $\underset{\sim}{\varepsilon} = (\varepsilon_x, \varepsilon_y, \gamma_{xy}, \gamma_{xz}, \gamma_{yz})^T$, respectively, and write the inverted elastic constitutive equations in the form

$$\underset{\sim}{\sigma} = \underset{\approx}{D} \, \underset{\sim}{\varepsilon}^e \quad . \tag{4.3}$$

It is convenient to partition (4.3) into flexural and shear components. Accordingly, we write

$$\underset{\sim}{\sigma}_f = \underset{\approx}{D}_f \, \underset{\approx}{\varepsilon}^e_f$$

$$\underset{\sim}{\sigma}_s = \underset{\approx}{D}_s \, \underset{\approx}{\varepsilon}^e_s \qquad (4.4)$$

where $\underset{\sim}{\sigma}_f = (\sigma_x, \sigma_y, \sigma_{xy})^T$, $\underset{\sim}{\sigma}_s = (\tau_{xz}, \tau_{yz})^T$, $\underset{\sim}{\varepsilon}^e_f = (\varepsilon^e_x, \varepsilon^e_y, \gamma^e_{xy})^T$ and $\underset{\sim}{\varepsilon}^e_s = (\gamma^e_{xz}, \gamma^e_{yz})^T$. The constitutive matrices of equation (3.6) are then

$$\underset{\approx}{D}_f = \frac{E}{(1-\nu^2)} \begin{bmatrix} 1 & \nu & 0 \\ \nu & 1 & 0 \\ 0 & 0 & \frac{1-\nu}{2} \end{bmatrix} \quad \text{and} \quad \underset{\approx}{D}_s = \frac{E}{2(1+\nu)} \begin{bmatrix} 1 & 0 \\ 0 & 1 \end{bmatrix} .$$

The yield condition, equation (2.12), reduces to the plane stress form

$$\phi = [\tfrac{1}{3} (\sigma_x^2 - \sigma_x \sigma_y + \sigma_y^2) + \sigma_{xy}^2]^{\frac{1}{2}} - k^{\frac{1}{2}} \qquad (4.5)$$

where

$$k = A + c \, W_p \quad .$$

The plastic work term W_p may now be written as

$$W_p = \int \underset{\sim}{\sigma}_f^T \, d\underset{\sim}{\varepsilon}^p \qquad (4.6)$$

where $\underset{\sim}{\sigma}_f = (\sigma_x, \sigma_y, \sigma_{xy})^T$ and $d\underset{\sim}{\varepsilon}^p = (d\varepsilon^p_x, d\varepsilon^p_y, d\gamma^p_{xy})$ are vectors of in-plane stresses and conjugate plastic strain increments, respectively.

4.3 Finite Element Discretisation

It is necessary first of all to perform the integration in (2.27). Defining an expression $\bar{W}^o_e$ for the e^{th} element of the assemblage as

$$\bar{W}^o_e = \frac{1}{2} D_{ijk\ell} \left(\dot{\varepsilon}_{ij} - \lambda \frac{\partial \phi}{\partial \sigma_{ij}}\right)\left(\dot{\varepsilon}_{k\ell} - \lambda \frac{\partial \phi}{\partial \sigma_{k\ell}}\right) + \frac{\lambda^2}{2G} \quad , \qquad (4.7)$$

we obtain

$$\int_V \bar{W}^o \, dV = \sum_{e=1}^{m} \int_{V_e} \bar{W}_e^o \, dV_e \tag{4.8}$$

for a body consisting of m elements, where V is the volume of the body and V_e the volume of the e^{th} element.

Using the ideas from the isoparametric formulation of the heterosis element we proceed to write the integration of equation (4.7) in matrix form. We will consider each term of (4.7) separately. The first term is

$$\int_{V_e} D_{ijk\ell} \, \dot{\varepsilon}_{ij} \, \dot{\varepsilon}_{k\ell} \, dV_e \quad , \tag{4.9}$$

which we recognise to be the conventional elastic strain energy term; according to the procedures discussed in Chapter 3 this may be written as

$$\int_{V_e} z^2 \, \dot{\underset{\sim}{\varepsilon}}_f^{eT} \, \underset{\approx}{D}_f \, \dot{\underset{\sim}{\varepsilon}}_f^{e} \, dV_e + \int_{V_e} \dot{\underset{\sim}{\varepsilon}}_s^{eT} \, \underset{\approx}{D}_s \, \dot{\underset{\sim}{\varepsilon}}_s^{e} \, dV_e \quad . \tag{4.10}$$

We can integrate through the thickness directly to obtain

$$\int_{A_e} \dot{\underset{\sim}{\varepsilon}}_f^{eT} \, \underset{\approx}{D}'_f \, \dot{\underset{\sim}{\varepsilon}}^{e} \, dA_e + \int_{A_e} \dot{\underset{\sim}{\varepsilon}}_s^{eT} \, \underset{\approx}{D}'_s \, \dot{\underset{\sim}{\varepsilon}}_s^{e} \, dA_e \tag{4.11}$$

where A_e is the area of the e^{th} element,

$$\underset{\approx}{D}'_f = \frac{Et^3}{12(1-\nu^2)} \begin{bmatrix} 1 & \nu & 0 \\ \nu & 1 & 0 \\ 0 & 0 & \frac{1-\nu}{2} \end{bmatrix}, \quad \underset{\approx}{D}'_s = (5/6) \frac{Et}{2(1+\nu)} \begin{bmatrix} 1 & 0 \\ 0 & 1 \end{bmatrix},$$

see previous page

and t is the thickness of the plate. Writing equation (3.10) in rate form we get

$$\begin{aligned} \dot{\underset{\sim}{\varepsilon}}^e_f &= \underset{\approx}{B}_f \, \dot{\underset{\sim}{d}}^e \quad , \\ \dot{\underset{\sim}{\varepsilon}}^e_s &= \underset{\approx}{B}_s \, \dot{\underset{\sim}{d}}^e \quad , \end{aligned} \tag{4.12}$$

where $\underset{\approx}{B}_f$ and $\underset{\approx}{B}_s$ are 3 x 26 rectangular matrices and $\dot{\underset{\sim}{d}}^e$ is the column vector of nodal degrees of freedom with 26 entries. Thus (4.11) becomes

$$\dot{\underset{\sim}{d}}^{eT} \left(\int_{A_e} \underset{\approx}{B}_f^T \, \underset{\approx}{D}'_f \, \underset{\approx}{B}_f \, dA_e \right) \dot{\underset{\sim}{d}}^e + \dot{\underset{\sim}{d}}^{eT} \left(\int_{A_e} \underset{\approx}{B}_s^T \, \underset{\approx}{D}'_s \, \underset{\approx}{B}_s \, dA_e \right) \dot{\underset{\sim}{d}}^e \quad . \tag{4.13}$$

Using the appropriate order of numerical intergration and noting that $dA_e = (\det J^e)\, d\xi\, d\eta$, where J^e is the standard element Jacobian matrix, we can write (4.13) as

$$\dot{\underset{\sim}{d}}^{eT} \, \underset{\approx}{K}^e_f \, \dot{\underset{\sim}{d}}^e + \dot{\underset{\sim}{d}}^{eT} \, \underset{\approx}{K}^e_s \, \dot{\underset{\sim}{d}}^e \tag{4.14}$$

where

$$\underset{\approx}{K}^e_f = \int_{A_e} \underset{\approx}{B}_f^T \, \underset{\approx}{D}'_f \, \underset{\approx}{B}_f \, dA_e$$

and

$$\underset{\approx}{K}^e_s = \int_{A_e} \underset{\approx}{B}_s^T \, \underset{\approx}{D}'_s \, \underset{\approx}{B}_s \, dA_e$$

are the flexural and shear contributions to the standard elastic element stiffness matrix.

The next term of the function which we consider is

$$- \int_{A_e} D_{ijk\ell} \, \dot{\varepsilon}_{ij} \, \lambda \, \frac{\partial \phi}{\partial \sigma_{k\ell}} \quad . \tag{4.15}$$

Again numerical integration is used to evaluate this volume integral and we exploit this procedure to associate a plastic multiplier with a particular integration point, pqr, i.e.

$$\dot{\underset{\sim}{\varepsilon}}^{p}_{pqr} = \lambda_{pqr} \left(\frac{\partial \phi}{\partial \underset{\sim}{\sigma}}\right)_{pqr} \tag{4.16}$$

where the subscript pqr indicates evaluation at the intergration point pqr, and

$$\dot{\underset{\sim}{\varepsilon}}^{p}_{pqr} = \left\{ \dot{\varepsilon}^{p}_{x} , \quad \dot{\varepsilon}^{p}_{y} , \quad \dot{\gamma}^{p}_{xy} \right\}^{T}_{pqr} ,$$

$$\frac{\partial \phi}{\partial \underset{\sim}{\sigma}}_{pqr} = \left\{ \frac{\partial \phi}{\partial \sigma_{x}} , \quad \frac{\partial \phi}{\partial \sigma_{y}} , \quad \frac{\partial \phi}{\partial \sigma_{xy}} \right\}^{T}_{pqr} .$$

Expression (4.15) is now written as

$$- \dot{\underset{\sim}{d}}^{e^{T}} \left(\sum_{p=1}^{f} \sum_{q=1}^{g} \sum_{r=1}^{h} \alpha_{pqr} Z_{r} \underset{\approx}{B}^{T}_{f_{pqr}} \underset{\approx}{D}_{f} \underset{\sim}{\beta}_{pqr} \det J^{e}_{pqr} \right) \lambda_{pqr} \tag{4.17}$$

where α_{pqr} is the numerical integration weighting factor and Z_{r} is the value of the z coordinate at integration point r. If we use a 3 x 3 gaussian scheme across the element, f = 3 and g = 3. For integration through the thickness we use a four point Newton-Cotes rule with two points on the plate surfaces, and so h = 4.

To avoid any numerical difficulties we normalise the gradient vector, i.e. we write

$$\underset{\sim}{\beta}' = \left\{ \left(\frac{\partial \phi}{\partial \sigma_{x}}\right)' , \quad \left(\frac{\partial \phi}{\partial \sigma_{y}}\right)' , \quad \left(\frac{\partial \phi}{\partial \sigma_{zy}}\right)' \right\}^{T} \tag{4.18}$$

where

$$\left(\frac{\partial\phi}{\partial\sigma_x}\right)' = \frac{\partial\phi}{\partial\sigma_x}\left[\left(\frac{\partial\phi}{\partial\sigma_x}\right)^2 + \left(\frac{\partial\phi}{\partial\sigma_y}\right)^2 + \left(\frac{\partial\phi}{\partial\sigma_{xy}}\right)^2\right]^{-\frac{1}{2}} \text{ etc.}$$

and introduce a weighted plastic multiplier λ' such that

$$\dot{\underset{\sim}{\varepsilon}}^p = \lambda' \left(\frac{\partial\phi}{\partial\underset{\sim}{\sigma}}\right)' \tag{4.19}$$

We now form a rectangular matrix

$$\underset{\approx}{A}^e = [\beta'_{111} \quad , \quad \beta'_{112} \quad \ldots\ \beta'_{fgh}]$$

of normalised gradient vectors and a column vector

$$\underset{\sim}{\lambda}'^e = \{\lambda'_{111} \quad , \quad \lambda'_{112} \quad , \quad \ldots\ \lambda'_{fgh}\}^T$$

of weighted plastic multipliers and write (4.17) as

$$-\dot{\underset{\sim}{d}}^{eT}\ \underset{\approx}{N}^{eT}\ \underset{\approx}{D}_f\ \underset{\approx}{A}^e\ \underset{\sim}{\lambda}'^e \quad . \tag{4.20}$$

Note that $\underset{\approx}{N}^e$ now contains the usual $\underset{\approx}{B}_f$ terms evaluated at specific gauss points plus the other terms of (4.19) associated with the numerical integration procedure.

The third term in the functional is

$$-\int_{V_e} D_{ijk\ell}\ \dot{\varepsilon}_{k\ell}\ \lambda\ \frac{\partial\phi}{\partial\sigma_{ij}}\ dV_e \tag{4.21}$$

and can be recognised as the transpose of (4.17), since $D_{ijk\ell} = D_{k\ell ij}$. Thus in matrix form we write

$$-\underset{\sim}{\lambda}'^{eT}\ \underset{\approx}{A}^{eT}\ \underset{\approx}{D}_f\ \underset{\approx}{N}^e\ \dot{\underset{\sim}{d}}^e \tag{4.22}$$

Using the same procedure as above we can write the fourth term of equation (4.7)

$$\int_{V_e} D_{ijk\ell} \lambda \frac{\partial \phi}{\partial \sigma_{ij}} \lambda \frac{\partial \phi}{\partial \sigma_{k\ell}} dV_e \tag{4.23}$$

as

$$\sum_{p=1}^{f} \sum_{q=1}^{g} \sum_{r=1}^{h} \alpha_{pqr} \lambda'_{pqr} \underset{\sim}{\beta}'^{T}_{pqr} \underset{\approx}{D}_f \underset{\sim}{\beta}'_{pqr} \lambda'_{pqr} \det J^e_{pqr} \tag{4.24}$$

or

$$\underset{\sim}{\lambda}'^{e^T} \underset{\approx}{A}^{e^T} \underset{\approx}{D}'_f \underset{\approx}{A}^e \underset{\sim}{\lambda}'^e \quad . \tag{4.25}$$

$\underset{\approx}{D}'_f$ now contains the weighting factor and det J^e_{pqr}.

The last term of (4.7) becomes

$$\int_{V_e} \frac{\lambda^2}{2G} dV_e \quad . \tag{4.26}$$

Recall from Chapter 2 that

$$1/G = E_p \left(\frac{\partial \phi}{\partial \sigma_{k\ell}} \frac{\partial \phi}{\partial \sigma_{k\ell}} \right) \tag{4.27}$$

Now using the weighted plastic multipliers we write (4.26) as

$$\sum_{p=1}^{f} \sum_{q=1}^{g} \sum_{r=1}^{h} \alpha_{pqr} \lambda'_{pqr} E_p \lambda'_{pqr} \det J^e_{pqr} = \underset{\sim}{\lambda}'^{e^T} \underset{\approx}{D}_p \underset{\sim}{\lambda}'^e \tag{4.28}$$

where $\underset{\approx}{D}_p$ is a diagonal matrix with E_p along the diagonal multiplied by the numerical integration constants.

The surface integral from equation (2.27)

$$\int_{S_{T_e}} \dot{T}_i \dot{u}_i \, dS_e \tag{4.29}$$

becomes, using standard finite element procedures,

$$\dot{\underset{\sim}{d}}^{e^T} \dot{\underset{\sim}{P}}^{e} \tag{4.30}$$

where $\dot{\underset{\sim}{P}}^{e}$ is the load vector. In this case care must be taken to ensure that the correct shape functions are used with the appropriate loading terms. Once all these terms have been evaluated we may assemble them to form the whole functional. Introducing a combined column vector $(\dot{\underset{\sim}{d}} \,\vdots\, \underset{\sim}{\lambda}')$ equation (4.8) in matrix form becomes

$$(\dot{\underset{\sim}{d}} \,\vdots\, \underset{\sim}{\lambda}')^T \underset{\approx}{K^*} (\dot{\underset{\sim}{d}} \,\vdots\, \underset{\sim}{\lambda}') \tag{4.31}$$

where the system matrix $\underset{\approx}{K^*}$ is

$$\underset{\approx}{K^*} = \left[\begin{array}{c:c} \underset{\approx}{B}_f^T \underset{\approx}{D}'_f \underset{\approx}{B}_f + \underset{\approx}{B}_s^T \underset{\approx}{D}'_s \underset{\approx}{B}_s & -\underset{\approx}{N}^T \underset{\approx}{D}_f \underset{\approx}{A} \\ \hdashline -\underset{\approx}{A}^T \underset{\approx}{D}_f \underset{\approx}{N} & \underset{\approx}{A}^T \underset{\approx}{D}_f \underset{\approx}{A} + \underset{\approx}{D}_p \end{array}\right] \tag{4.32}$$

Note that $\underset{\approx}{K^*}$ is symmetric.

In the absence of body forces the functional, equation (2.27), becomes

$$\bar{U}_p^o = \frac{1}{2} (\dot{\underset{\sim}{d}} \,\vdots\, \underset{\sim}{\lambda}')^T \underset{\approx}{K^*} (\dot{\underset{\sim}{d}} \,\vdots\, \underset{\sim}{\lambda}') - (\dot{\underset{\sim}{d}} \,\vdots\, \underset{\sim}{\lambda}')^T (\dot{\underset{\sim}{P}} \,\vdots\, \underset{\sim}{0}) \tag{4.33}$$

The numerical solution to a particular rate problem is then given by that value of $(\dot{\underset{\sim}{d}} \,\vdots\, \underset{\sim}{\lambda}')$ which minimises equation (4.33) subject to the following constraints: for every λ'_{pqr} in $\underset{\sim}{\lambda}'$

either $\quad \lambda'_{pqr} = 0 \quad$ if $\quad \phi_{pqr} < 0$ (4.34a)

or $\quad \lambda'_{pqr} \geq 0 \quad$ if $\quad \phi_{pqr} = 0$ (4.34b)

Since $\bar{U}_p^o$ is homogeneous in the rates we may determine the solution to the incremental problem by using $(\Delta\underset{\sim}{d} \,;\, \underset{\sim}{\lambda})$ and $(\Delta\underset{\sim}{P} \,;\, \underset{\sim}{0})$ instead of their rate form; here $\Delta(\ )$ denotes the increment in a quantity.

We can state the solution to (4.33) as a formal quadratic programming problem: defining a vector $\underset{\sim}{\phi}$ which contains the magnitudes of the yield function at the gauss points, the quadratic programming problem is

$$\min \{ \bar{U}_p^o (\Delta\underset{\sim}{d}, \lambda') \mid \underset{\sim}{\lambda}' \geq 0, \quad \underset{\sim}{\phi}^T \underset{\sim}{\lambda}' = 0 \} \tag{4.35}$$

If equation (4.37) is solved by means of standard programming algorithms the computer time would be prohibitive for any realistic problem, particularly as it must be solved at each incremental step. Some alternative solution procedure is therefore desirable.

A simple intuitive numerical algorithm based on the constraints of (4.34) was suggested by Martin and Reddy (1977) and used successfully by Dittmer (1978) for plane problems. This algorithm will be presented in the next section and the general numerical procedure for the incremental problem is discussed in the last section.

4.4 An Algorithm for the Minimisation of $\bar{U}_p^o$.

Suppose that the load vector $\underset{\sim}{P}$ is known at a certain stage of loading programme. The displacements, elastic and plastic strains and the stresses corresponding to $\underset{\sim}{P}$ are known. We assume there are at least some non-zero plastic strains. For the solution to the next load increment $\Delta\underset{\sim}{P}$, we are required to minimize the incremental form of equation (4.33) subject to the constraints of equation (4.34).

We divide the gauss points of the plate into two groups. The gauss points governed by constraint (4.34a) are elastic and said to be in V_e. Those governed by constraint (4.34b) are said to be in V_p. However, we do not know *a priori* whether the latter will load plastically or unload elastically. We note that if all the components of $(\underset{\sim}{\Delta d} \,\vdots\, \underset{\sim}{\lambda'})$ are non-zero the least value of the functional is given by the solution of the set of simultaneous linear equations

$$\underset{\approx}{K^*}\ (\underset{\sim}{\Delta d} \,\vdots\, \underset{\sim}{\lambda'}) \;=\; (\underset{\sim}{\Delta P} \,\vdots\, \underset{\sim}{0}) \quad . \tag{4.36}$$

This suggests an algorithm for the minimization of $\bar{U}_p^o$ based on an initial guess as to which elements of $\underset{\sim}{\lambda'}$ in V_p will load plastically; the elements of $\underset{\sim}{\lambda'}$ which are in V_e are all obviously zero.

We proceed as follows : we identify the gauss points in V_e and those in V_p for which unloading is *assumed* to occur and eliminate the corresponding rows and columns of $\underset{\approx}{K^*}$. The remaining equations of (4.36) are solved for $\underset{\sim}{\Delta d}$ and the non-zero components of $\underset{\sim}{\lambda'}$. This represents a trial solution for $\underset{\sim}{\Delta d}$ and $\underset{\sim}{\lambda'}$.

We now consider the Gauss points in V_p. If, at Gauss point pqr λ'_{pqr} was assumed non-zero and

$$\lambda'_{pqr} \geq 0$$

or for Gauss point pqr λ'_{pqr} was assumed zero and

$$\left(\frac{\partial \phi}{\partial \underset{\sim}{\sigma}}\right)'_{pqr} \Delta\underset{\sim}{\sigma}_{pqr} < 0$$

we have found the correct solution. If these checks are not satisfied we must revise the choice of components in V_p assumed zero or non-zero,

and resolve equation (4.36). This we do by considering the components of $\underset{\sim}{\lambda}'$ that failed the checks. If they were assumed either zero or non-zero they are now assumed non-zero, respectively.

Convergence of this iterative procedure has not been conclusively proved, but experience by Martin and Reddy (1977) and Dittmer (1978) indicates that it is rapid and fails only as the limit load is approached in the elastic-perfectly plastic case. In the case of monotonically increasing loads, unloading seldom occurs and the best initial guess in the algorithm is that the components of $\underset{\sim}{\lambda}'$ in the V_p are non-zero. Even in the non-monotonic loading situation this initial guess leads to convergence within one or two iterations.

It has been shown by Dittmer (1978) that, in the context of plane stress or strain, the set of equations (4.36) reduces to the conventional tangent modulus approach for incremental elastic-plastic analysis.

4.5 Incremental Solution Procedure

The incremental solution proceeds as follows: for the body under consideration we determine which components of $\underset{\sim}{\lambda}'$ are in V_p and non-zero. The next load increment is applied and the resulting set of equations is then solved for displacement increments and plastic multipliers. The minimization algorithm of the preceding section is employed to determine whether we have obtained the correct solution or not. However, if a point in the body which was in V_e passes into V_p the *load increment* must be scaled down accordingly, to ensure that the point just

reaches its yield value. The body will be in equilibrium at this stage. The augmented stiffness matrix $\underset{\approx}{K}^*$ must now be reformulated before any more load can be applied to the body. We note that the number of load step increments depends on the number of gauss points that go plastic. This places a restriction on the loading programme. Symmetry may reduce the number of steps, but the procedure is still rather cumbersome.

An alternative procedure is to allow material points initially in V_e, to enter V_p, and to calculate the plastic strains that have occurred in some other manner. Thus a set incremental step can be applied at an arbitrary stage in the loading programme. The plastic strains associated with the non-zero λ' in V_p at the start of the step are calculated in the usual manner. However, we now make use of the elastic-plastic state determination schemes used in the tangent modulus approach, to calculate the plastic strains for the points that were in V_e at the start of the load increments, but which have now entered V_p. It is obvious that some sort of iterative scheme is now necessary to restore equilibrium to the system.

The numerical implementation of the incremental procedure will be discussed in Chapter 6. However, we first introduce the two elastic-plastic state determination schemes used in this study, in the next chapter.

CHAPTER 5

ELASTIC-PLASTIC STATE DETERMINATION SCHEMES

5.1 Introduction

In conventional incremental elastic-plastic finite element programmes the calculation of plastic strain increments is crucial to the accuracy of the solution. The corresponding stress increment can then be found. Provided the constitutive equations are satisfied any out of balance load, usually due to some stress adjustment, can be accommodated through successive iteration, provided the limit load, if present, is not exceeded. For the displacement based finite element method the problem may be stated as follows: given a total strain increment, calculate the corresponding stress increment. This ensures that the compatibility conditions are not violated. It is important to keep any error in this calculation as small as possible as it may be done a considerable number of times during any normal loading programme. An efficient and accurate scheme is thus desirable.

In the present study if we apply an arbitrary load step at any given stage of the loading programme, some points initially elastic may become plastic. However, in the formulation of the augmented stiffness matrix (4.32) the plastic strains that will occur at these points have not been accounted for. The above procedure is now used to obtain the plastic strain increments instead of adjusting the load step and reformulating the augmented stiffness matrix. The two schemes used in this study are the elastic predictor-radial corrector method and the tangent predictor-radial return method discussed by Schreyer,

Kulak and Kramer (1979). However, whereas they present the plane stress problem explicitly, we will show that this can be done in an analogous manner to the fully three-dimensional case.

In the next section we first introduce some of the basic notation and equations that we will use for the invariant and deviatoric presentation. The final two sections are devoted to the two state determination schemes. The manner in which these schemes are implemented is discussed in Chapter 6.

5.2 General Equations

As stated in section 4.2 we can regard the elastic-plastic behaviour of the plate as a problem in plane stress. A convenient notation for writing the plasticity equations for plane problems has been given by Martin (1982). This enables us to manipulate the plane stress equations using deviatoric and invariant quantities in the same manner as for the fully three-dimensional case. Consider the elastic flexural part of equation (4.4) :

$$\underset{\sim}{\sigma}_f = \underset{\approx}{D}_f \, \underset{\sim}{\varepsilon}^e_f \tag{5.1}$$

where

$$\underset{\sim}{\sigma}_f = (\sigma_{11}, \sigma_{22}, \sigma_{12})^T = (\sigma_x, \sigma_y, \sigma_{xy})^T \quad ,$$

$$\underset{\sim}{\varepsilon}^e_f = (\varepsilon^e_{11}, \varepsilon^e_{22}, \gamma^e_{12})^T = (\varepsilon^e_x, \varepsilon^e_y, \gamma^e_{xy})^T \quad .$$

The components of the stress deviator s_{ij} are

$$\begin{aligned} s_{11} &= {}^{2}/_{3}\,\sigma_{11} - {}^{1}/_{3}\,\sigma_{22} \quad , \\ s_{22} &= -{}^{1}/_{3}\,\sigma_{11} + {}^{2}/_{3}\,\sigma_{22} \quad , \\ s_{33} &= -{}^{1}/_{3}\,\sigma_{11} - {}^{1}/_{3}\,\sigma_{22} \quad , \\ s_{12} &= \sigma_{12} \quad . \end{aligned} \tag{5.2}$$

The components of the strain deviator e_{ij} are

$$\begin{aligned} e_{11} &= {}^{2}/_{3}\,\varepsilon_{11} - {}^{1}/_{3}\,\varepsilon_{22} \quad , \\ e_{22} &= -{}^{1}/_{3}\,\varepsilon_{11} + {}^{2}/_{3}\,\varepsilon_{22} \quad , \\ e_{33} &= -{}^{1}/_{3}\,\varepsilon_{11} - {}^{1}/_{3}\,\varepsilon_{11} \quad , \\ e_{12} &= \varepsilon_{12} \quad . \end{aligned} \tag{5.3}$$

We note that $s_{11} + s_{22} + s_{33} = 0$ and introduce the vector

$$\underset{\sim}{s} = (s_{11}, s_{22}, s_{12})^{T} \tag{5.4}$$

Now we write the effective shear stress of equation (2.12) as

$$s = \sqrt{{}^{1}/_{2}\ \underset{\sim}{s}^{T}\ \underset{\approx}{n}\ \underset{\sim}{s}} \tag{5.5}$$

where

$$\underset{\approx}{n} = \begin{bmatrix} 2 & 1 & 0 \\ 1 & 2 & 0 \\ 0 & 0 & 2 \end{bmatrix}$$

The effective shear stress rate is then given by

$$\dot{s} = \frac{1}{2s} \underset{\sim}{s}^T \underset{\approx}{n} \dot{\underset{\sim}{s}} \quad . \tag{5.6}$$

To define an effective shear strain rate $\dot{e}$ we use the strain deviatoric components and introduce the deviatoric strain rate vector

$$\dot{\underset{\sim}{e}} = (\dot{e}_{11}, \dot{e}_{22}, \dot{e}_{12})^T \tag{5.7}$$

and define

$$\dot{e} = {}^1/_s \, \dot{\underset{\sim}{e}}^T \underset{\approx}{n} \underset{\sim}{s} \quad . \tag{5.8}$$

Thus we can write the elastic rate equations in terms of deviatoric components as

$$\dot{\underset{\sim}{s}} = 2 G \dot{\underset{\sim}{e}} \tag{5.9}$$

and, in terms of invariants,

$$\dot{s} = G \dot{e} \quad , \tag{5.10}$$

where $G = E/2(1+\nu)$ is the shear modulus. It can be shown that equation (5.10) reduces to equation (5.1).

As stated in chapter 2, we use a von Mises yield criterion with isotropic hardening. From equation (5.5) we can write the yield function $\phi(\sigma, W_p)$ in terms of deviatoric components as

$$\phi = \sqrt{\tfrac{1}{2} \underset{\sim}{s}^T \underset{\approx}{n} \underset{\sim}{s}} - k^{\frac{1}{2}} \tag{5.11}$$

where

$$k = A + cW_p \quad ,$$

$$W_p = \int \underset{\sim}{s}^T \underset{\approx}{n} \, d \, \underset{\sim}{e}^p \quad .$$

W_p is the plastic work term, A is some initial yield value and c is a constant. In invariant form (5.11) becomes

$$\phi(s, W_p) = s - k^{\frac{1}{2}} \tag{5.12}$$

where W_p is written as

$$W_p = \int s \, d \, e^p \quad . \tag{5.13}$$

The plastic strain rate given by equation (2.10) is

$$\dot{\underset{\sim}{\varepsilon}}^p = \lambda \frac{\partial \phi}{\partial \underset{\sim}{\sigma}} \quad . \tag{5.14}$$

To ensure that we relate conjugate quantities, we write

$$\dot{\underset{\sim}{e}}^p = \lambda \frac{\partial \phi}{\partial s} \frac{\partial s}{\partial (\underset{\approx\sim}{ns})} = \frac{\lambda}{2s} \frac{\partial \phi}{\partial s} \underset{\sim}{s} \quad . \tag{5.15}$$

Premultiplying equation (5.14) by $\frac{1}{s} \underset{\sim}{s}^T \underset{\approx}{n}$ we get

$$\dot{e}^p = \lambda \frac{\partial \phi}{\partial s} \quad . \tag{5.16}$$

The total strain may be divided into elastic and plastic parts. Thus we can write

$$\dot{\underset{\sim}{e}} = \dot{\underset{\sim}{e}}^e + \dot{\underset{\sim}{e}}^p \tag{5.17}$$

or

$$\dot{e} = \dot{e}^e + \dot{e}^p \quad . \tag{5.18}$$

For elastic-plastic behaviour equation (5.10) becomes

$$\dot{s} = G(\dot{e} - \dot{e}^p) \tag{5.19}$$

From equation (5.13) we obtain

$$\dot{W}_p = s\,\dot{e}^p \tag{5.20}$$

and from equations (5.16) and (5.12) we get

$$\dot{e}^p = \lambda \quad . \tag{5.21}$$

Noting that $k^{\frac{1}{2}} \equiv k(W_p)^{\frac{1}{2}}$, for loading, i.e. $\phi = 0$, $\dot{\phi} = 0$, we have from equation (5.12)

$$\dot{s} - \tfrac{1}{2} k^{-\frac{1}{2}} \frac{dk}{dW_p} \dot{W}_p = 0 \tag{5.22}$$

Substituting from equations (5.18), (5.19), (5.20) and $\frac{dk}{dW_p} = c$ we get

$$G\dot{e} - G\lambda - \tfrac{1}{2} k^{-\frac{1}{2}} c\, s\, \lambda = 0 \tag{5.23}$$

or

$$\lambda = \frac{G\dot{e}}{G + c/2} \quad . \tag{5.24}$$

Now consider an arbitrary material point which is initially elastic, and suppose that after applying an increment of load we obtain an increment in plastic strain at this point, i.e.

$$\phi_o < 0 \quad , \qquad \dot{\phi} = 0 \tag{5.25}$$

or

$$s_o - k_o^{\frac{1}{2}} < 0 \quad , \qquad s - k^{\frac{1}{2}} = 0 \tag{5.26}$$

Here, ϕ_o and ϕ indicate the initial and final values of the yield function. We can write the second expression of (5.26) as

$$(s_o + \Delta s) - k\,(W_p^o + \Delta W_p)^{\frac{1}{2}} = 0 \qquad (5.27)$$

and expanding the second term in a Taylor series, retaining terms up to first order, we obtain

$$s_o + \Delta s - k(W_p^o)^{\frac{1}{2}} - k(W_p)^{-\frac{1}{2}} \frac{dk}{dW_p}\,\Delta W_p = 0 \quad . \qquad (5.28)$$

Substitution of the incremental form of equations (5.19), (5.20) and (5.21) in equation (5.28) yields

$$s_o - k_o^{\frac{1}{2}} + G\Delta e - G\lambda - \tfrac{1}{2}\,c\lambda = 0 \qquad (5.29)$$

or

$$\lambda = \frac{G\Delta e + (s_o - k_o^{\frac{1}{2}})}{G + {}^{c}/_{2}} \quad . \qquad (5.30)$$

Note the similarity between equations (5.24) and (5.30) .

From (5.29) it follows that

$$s_f = k_o^{\frac{1}{2}} + \tfrac{1}{2}\,c\lambda \quad . \qquad (5.31)$$

5.3 Elastic Predictor-Radial Corrector Method

In this method we start at a stress point within the yield surface. For the next increment in strain we assume elastic behaviour to calculate the stress increment. If the stress point is still within the yield surface we proceed to the next step. If we have exceeded the yield value we adjust the stress increment by calculating the plastic strains that obviously have occurred and correct the stresses radially

so that at the end of the calculation, the stress point lies on the yield surface.

The crucial part of the calculation is the integration of equation (5.14). For the elastic predictor-radial corrector method we use a one step Euler backward scheme. As we are working in deviatoric space, from equation (5.15) we have

$$\Delta \underset{\sim}{e}^{p} = \lambda \frac{\underset{\sim}{s}_f}{2s_f} \tag{5.32}$$

where $\underset{\sim}{s}_f$ and s_f are the final values of the deviatoric stresses and effective shear stress, respectively. Assuming elastic behaviour we get

$$\underset{\sim}{s}_t = \underset{\sim}{s}_o + 2G\Delta \underset{\sim}{e} \tag{5.33}$$

where $\underset{\sim}{s}_o$ is the initial value of stress and $\Delta \underset{\sim}{e}$ the total strain increment. Using equations (5.19), (5.30) and (5.33) we write

$$\underset{\sim}{s}_f = \underset{\sim}{s}_t - G\lambda \frac{\underset{\sim}{s}_f}{s_f} \quad . \tag{5.34}$$

Rewriting, we obtain the final stress state in terms of the initial elastic prediction and the plastic strain increment, so that

$$\underset{\sim}{s}_f = \underset{\sim}{s}_t \Big/ \left(1 + G \frac{\lambda}{s_f}\right) \tag{5.35}$$

where λ is found from equation (5.30) and s_f from equation (5.31). If the stress increment is too large some error may be evident which can be reduced by applying equation (5.35) using smaller subincrements. The problem of when and how to subincrement has been dealt with by numerous authors. We will discuss the scheme implemented in chapter 6.

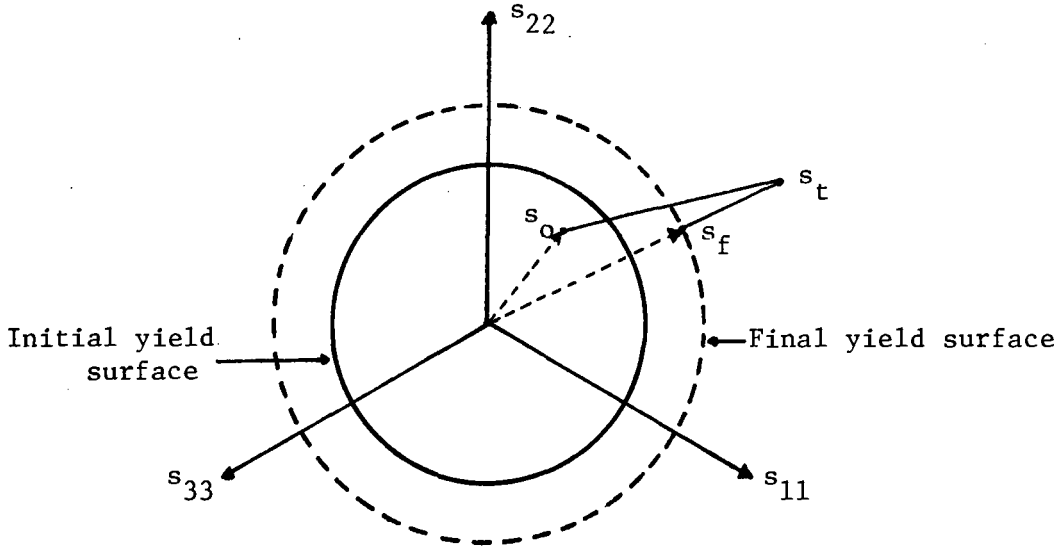

Figure 5.1 Elastic Predictor-Radial Corrector

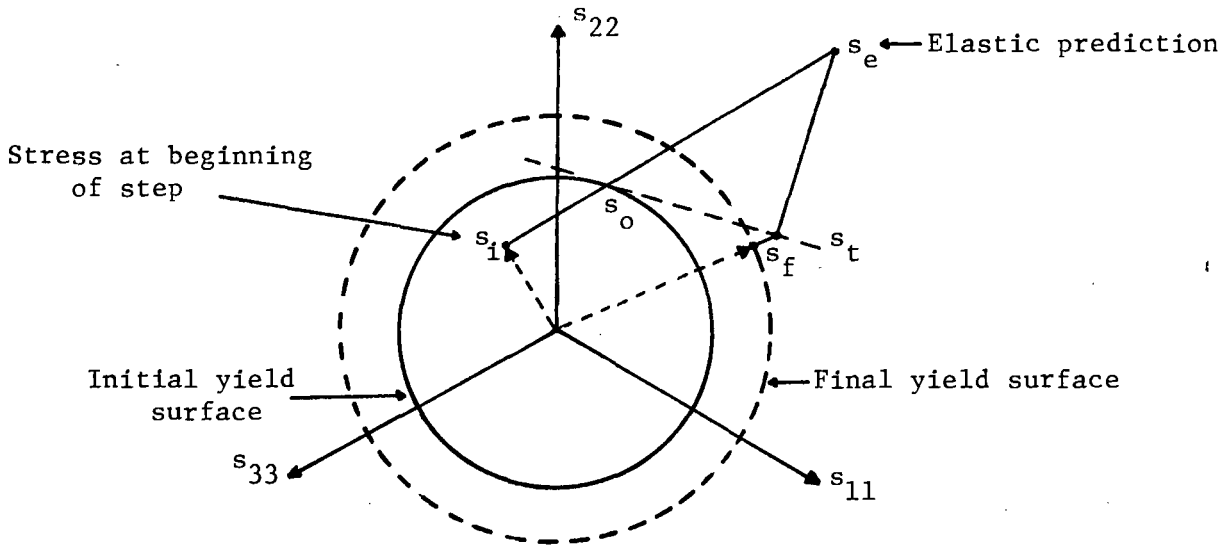

Figure 5.2 Tangent Predictor-Radial Return.

5.4 Tangent Predictor-Radial Return Method

For this method we proceed as for the radial corrector method. However, whereas the previous method is a one-step procedure, here we divide the step that takes the stress point into the elastic-plastic range into two parts. We scale the elastic increment so that the stress point just lies on the yield surface. The remainder of the stress is now adjusted to take into account plastic strains.

In this case we use an Euler forward scheme to integrate equation (5.15), i.e.

$$\dot{\underset{\sim}{e}}^p = \lambda \frac{\underset{\sim o}{s}}{2s_o} \tag{5.36}$$

where $\underset{\sim o}{s}$ and s_o are now the respective stress quantities calculated from the initial stresses on the yield surface.

The trail state of stress $\underset{\sim t}{s}$ is then found from

$$\underset{\sim t}{s} = \underset{\sim o}{s} + 2\,G\,\dot{\underset{\sim}{e}} - 2\,G\,\dot{\underset{\sim}{e}}^p \quad . \tag{5.37}$$

Substituting for equation (5.36) we get

$$\underset{\sim t}{s} = \underset{\sim o}{s} + G\,\dot{\underset{\sim}{e}} - G\,\frac{\underset{\sim o}{s}}{s_o} \tag{5.38}$$

and using equations (5.25) and (5.8) we obtain

$$\underset{\sim t}{s} = \underset{\sim o}{s} + \left[2\,G\,\underset{\approx}{I} - \frac{G^2}{G + c_{/2}}\,\frac{\underset{\sim o}{s}\,\underset{\sim o}{s}^T\,\underset{\sim}{n}}{s_o^2}\right]\dot{\underset{\sim}{e}} \tag{5.39}$$

where $\underset{\approx}{I}$ is the identity matrix.

In general $\underset{\sim}{s}_t$ will not lie on the yield surface and the stresses must be adjusted radially. As only the stresses are changed and not the plastic strains, there will be some non-compatibility. However, this error is very small. Thus the final stresses are given by

$$\underset{\sim}{s}_f = \left(s_f/s_t\right) \underset{\sim}{s}_t \tag{5.40}$$

where s_f is obtained from equation (5.31). If the stress increment is too great the amount that the stresses must be scaled radially back to the yield surface will be too great and a subincremation scheme must again be used.

CHAPTER 6

NUMERICAL IMPLEMENTATION

6.1 Introduction

A computer program has been written to analyse elastic-plastic plates based on the procedures outlined in the previous chapters. Although similar to the isoparametric formulations for the tangent modulus approach, there are certain obvious differences, e.g. the appearance of an augmented stiffness matrix in the present formulation. The program contains three basic levels in the solution procedure: the incremental problem, involving the solution of a set of simultaneous equations; the algorithm to check the kinematic constraints; and the equilibrium iterations necessary through the use of the elastic-plastic state determination schemes. The first two aspects are closely related and form the solution to the rate problem.

In the next section we discuss the formation of the augmented stiffness matrix and the numerical considerations in the solution of the resulting set of linear equations. The following two sections deal with the two incremental solution techniques. The first is what constitutes the 'exact' solution to the rate problem in which the load increment is scaled for each gauss point entering V_p. For the second technique a set load step is specified and the state determination schemes employed to calculate plastic strains for those points not included in V_p, but which have entered V_p in the current load step.

6.2 Formation of $\underset{\approx}{K}^*$ and the solution of $\underset{\approx}{K}^*(\Delta d \,|\, \lambda') = (\Delta P \,|\, 0)$

Recall the composition of $\underset{\approx}{K}^*$ from (4.32). The top left sub-matrix is the usual elastic stiffness matrix for a system and has only to be calculated once during the solution procedure. This is done in the initial stages of the program (see flow-chart (6.5)) using the selected reduced gaussian quadrature scheme discussed earlier. The remaining rows and columns of $\underset{\approx}{K}^*$ refer directly to individual plastic multipliers λ' associated with the numerical integration points. The number and value of these terms is determined by the plastic state of the body and must be recalculated at least at every incremental step. Therefore, for a particular integration point, pqr, we form the column vector $\underset{\approx pqr}{N^{e}}^{T}\ \underset{\approx f}{D}\ \underset{\sim pqr}{\beta'}$, its transpose, the appropriate terms from (4.25) and (4.28), and we place them in their corresponding locations in $\underset{\approx}{K}^*$. At the start of the solution $\underset{\approx}{K}^*$ will only be the elastic stiffness matrix. As the solution proceeds the additional rows and columns corresponding to the plastic regions of the body are included.

The profile solver of Wilson, Bathe and Doherty (1974) is especially suited for this type of analysis. It is based on the gauss elimination technique which seems the most efficient scheme for the solution of simultaneous equations. Only the non-zero components of the upper triangle of the factorised matrix are stored. This gives the matrix a 'sky-line' appearance, caused by the varying heights of the columns. The main advantage of this solver is that the factorisation proceeds column by column. We make use of this feature to factorise the elastic stiffness matrix at the start of the solution only. Then, during any step in which additional rows and columns are required to

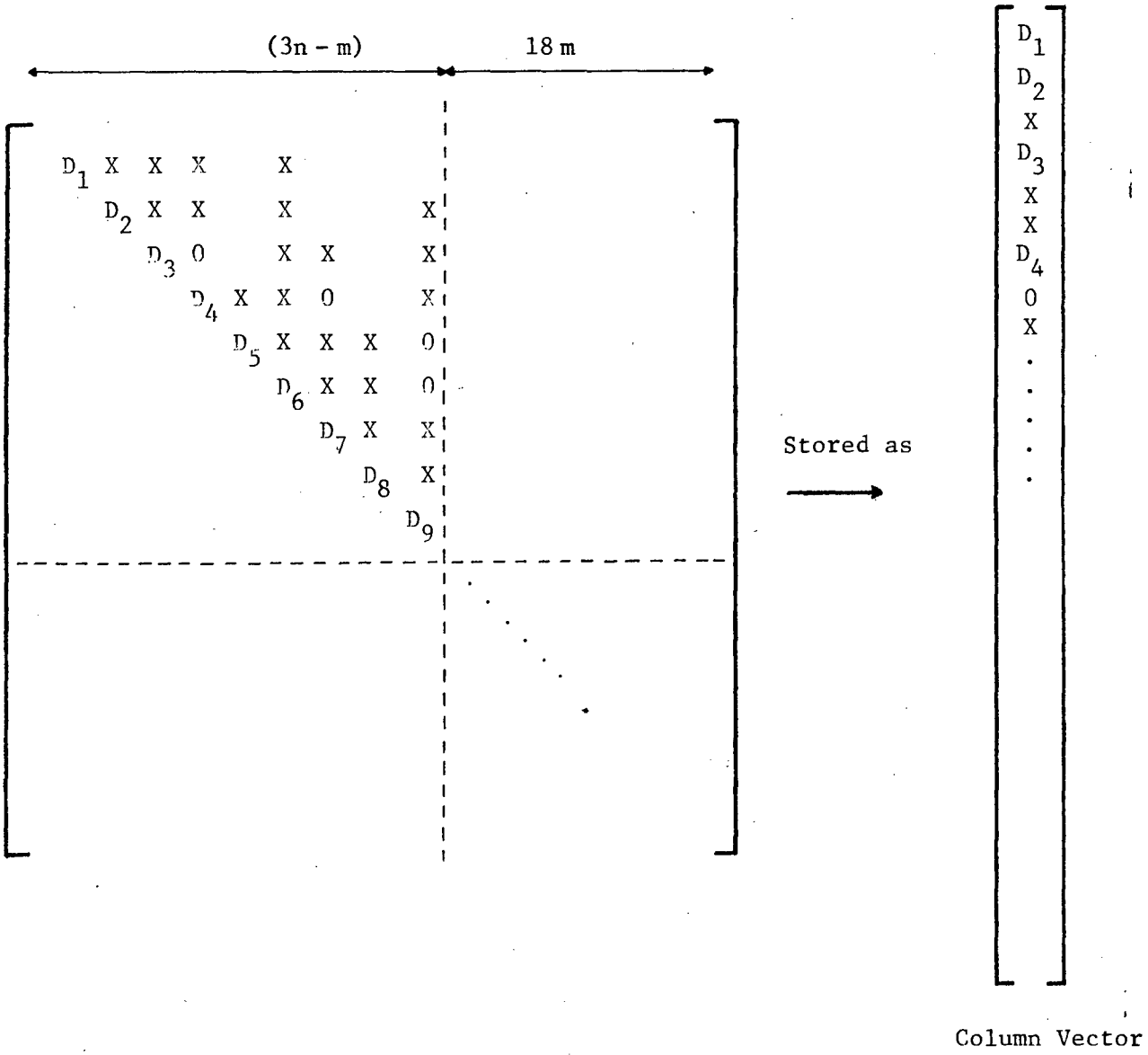

Figure 6.1 Profile Solver Storage Scheme for $\underset{\approx}{K}^*$

describe plastic behaviour, the relevant columns are added to the stiffness matrix and factorised individually. All redundant calculations during the solution of (4.36) are therefore eliminated.

For a body with m elements and n nodes the full $\underset{\approx}{K}^*$ matrix will be a $[(3n-m)+36m]x[(3n-m)+36m]$ square matrix, assuming that a $3 \times 3 \times 4$ numerical integration scheme is used. In the absence of in-plane forces the bending of the plate is symmetrical about the mid-plane and $\underset{\approx}{K}^*$ reduces to a $[(3n-m)+18m] \times [(3n-m)+18]$ matrix. In addition, all the displacement degrees of freedom that are constrained to zero are not included in the storage of $\underset{\approx}{K}^*$ for the profile solver. $\underset{\approx}{K}^*$ is stored as a column vector and certain housekeeping arrays containing column heights and the addresses of the diagonal terms are required, Bathe and Wilson (1976).

If $\underset{\approx}{K}^*$ becomes too large, e.g. for a body that has a large plastic region, to keep the amount of core storage down, $\underset{\approx}{K}^*$ can be divided into blocks which are then stored out of core. The solution then proceeds block by block.

6.3 Procedures for incremental solution involving a scaled load vector

As stated in Chapter 4 the incremental solution of the rate problem necessitates the adjustment of the load step increment so that each gauss point goes plastic in discrete steps. We proceed as follows: at an arbitrary stage in the solution we assume the body and the applied forces to be in equilibrium and all the stresses, plastic strains and reactions known. We now apply the remainder of the load (only relative magnitudes are required) and solve for the displacements and non-zero plastic multipliers. After the solution satisfying the constraints (4.34) has been obtained we calculate the stress and strain increments $\Delta\sigma_{ij}$ and $\Delta\varepsilon_{ij}$ corresponding to the applied load increment.

For each of the gauss points in V_e, i.e. $\phi(\sigma_{ij}, W_p) < 0$ we determine a factor ρ such that $\phi(\sigma_{ij} + \rho\Delta\sigma_{ij}, W_p) = 0$. The load vector is then scaled by the lowest value ρ_{min} of ρ obtained. As we have assumed linear behaviour all relevant quantities are also scaled by this amount and we have the solution for the current load increment. The gauss point for which $\rho = \rho_{min}$ is now included in V_p for the next load increment. This process is repeated until the loading programme has been completed or the limit load reached.

To calculate ρ, (Dittmer (1978)), we use the expression for the yield surface, equation (2.12),

$$\phi = \{ \frac{1}{3} [(\sigma_{ij} + \rho\Delta\sigma_{ij})(\sigma_{ij} + \rho\Delta\sigma_{ij}) - \frac{1}{3} (\sigma_{kk} + \rho\sigma_{\ell\ell})^2]\}^{\frac{1}{2}} - k^{\frac{1}{2}} = 0 \quad (6.1)$$

and rewrite it as

$$\frac{1}{3} [(\sigma_{ij} + \rho\Delta\sigma_{ij})(\sigma_{ij} + \rho\Delta\sigma_{ij}) - \frac{1}{3} (\sigma_{kk} + \rho\sigma_{\ell\ell})^2] - k = 0 \quad (6.2)$$

Obviously only the non-zero components of σ_{ij} appear in the actual calculation. Expanding equation (6.2) we use

$$\phi^*(\alpha,\beta) = \frac{1}{3} [\alpha_{ij}\beta_{ij} - \frac{1}{3} \alpha_{kk}\beta_{\ell\ell}] \quad (6.3)$$

to obtain

$$\rho^2 \phi^*(\Delta\sigma,\Delta\sigma) + 2\rho\phi^*(\sigma,\Delta\sigma) + \phi^*(\sigma,\sigma) - k = 0 \quad (6.4)$$

Since $\phi^*(\sigma,\Delta\sigma)$ and $\phi^*(\sigma,\sigma)$ are non-negative and $\phi^*(\Delta\sigma,\Delta\sigma)$ is always greater than zero, the positive root of equation (6.4) is given by

$$\rho = \frac{-\phi^*(\sigma,\Delta\sigma) + \sqrt{[\phi^*(\sigma,\Delta\sigma)]^2 - \phi^*(\Delta\sigma,\Delta\sigma)[\phi^*(\sigma,\sigma) - k]}}{\phi^*(\Delta\sigma,\Delta\sigma)} \quad (6.5)$$

In the determination of ρ_{min} values at some of the other gauss points

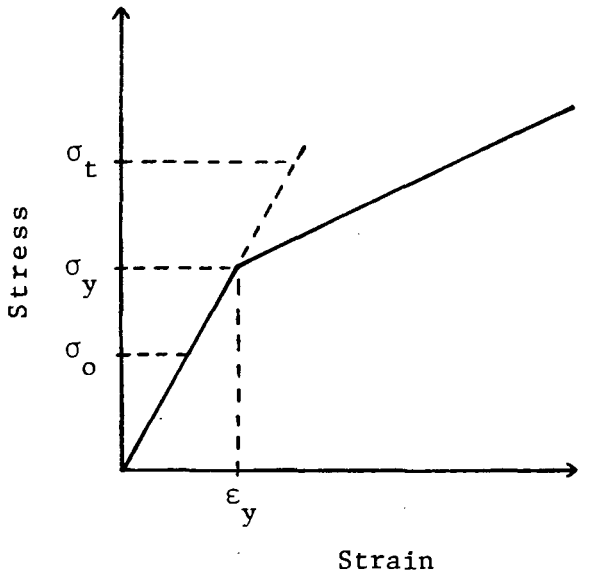

$$R = \frac{\sigma_y - \sigma_o}{\sigma_t - \sigma_o}$$

R = Scaling factor

Figure 6.2 One Dimensional Representation of Scaling Factor Calculation.

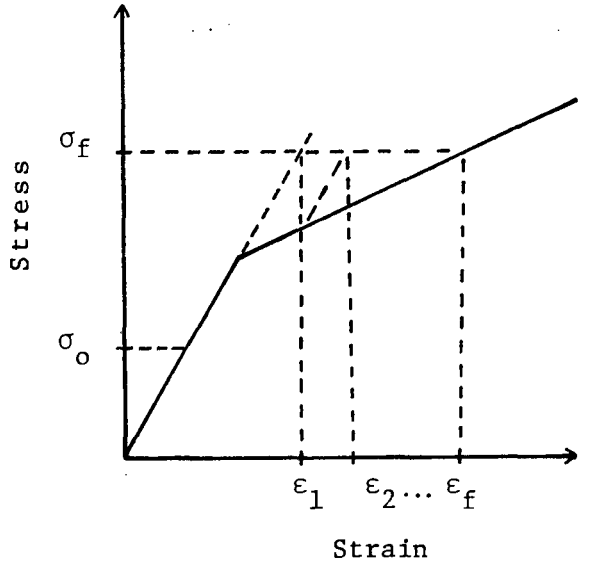

Figure 6.3 One Dimensional Representation of Iterative Process for Fixed Load Step.

may be close to ρ_{min}. For computational efficiency, any gauss point for which the value of ρ is within .1% of ρ_{min} is included in V_p for the next load increment. At the end of each incremental step the residual loads are calculated. Any residual load is then included in the load vector for the next increment. The residual loads for the above incremental solution procedure should be small and due mainly to our assumption to include the gauss points in V_p with ρ close to ρ_{min}. A force or energy norm may be used to measure the 'amount of out-of-balance' due to the residual loads. If this is above a certain tolerance we iterate until the norm is within the specified tolerance before proceeding to the next load increment.

For the elastic, perfectly plastic case the points on the yield surface tend to move off the yield surface at a tangent. This results in an inadmissable state of stress, $\phi > 0$. The stresses are adjusted radially back onto the yield surface by a simple scaling procedure. Any associated change in plastic strains is not accounted for, but this leads to a negligible error. The stresses and applied loads will, however, not be in equilibrium. To maintain equilibrium we again calculate the residual loads and include them in the load vector for the next step. As above, to ensure that the residual load does not become too large, an equilibrium iteration may be necessary before proceeding.

6.4 Implementation of the Elastic-Plastic State Determination Schemes

An alternative to the incremental procedure discussed in 6.3 is to apply a set incremental step size, and to use the state determination schemes of Chapter 5 to calculate certain of the plastic strains.

A more efficient solution is now obtained as the augmented stiffness matrix $\underset{\approx}{K}^*$ is re-calculated and factorised less often. To implement these schemes we proceed in the same manner as in the first part of section 6.3. However, here the load step is kept fixed. The solution to the rate problem, once the constraints (4.34) are satisfied, is valid, but the yield condition is violated for those gauss points that were in V_e and have entered V_p, during the application of the current load step. We now use the state determination schemes to calculate the plastic strains that have occurred for these points, and adjust the stresses accordingly, so that the yield condition is satisfied. For those points in V_p at the beginning of the step, the plastic strains are obtained from the plastic multipliers solved for.

It is obvious now, since some stresses have been brought back to the yield surface, that the equivalent nodal loads given by

$$\int_V \underset{\approx}{B}_f^T \underset{\sim}{\sigma}_f \, dV \tag{6.6}$$

and the applied loads will not be in equilibrium. The difference between the aforementioned loads is compared relative to an appropriate norm to determine whether or not the error is acceptable. If not, we iterate until a converged solution has been obtained.

At this stage there are two options available: we apply the residual loads as a load vector and either (1) solve for displacements etc. from the original set of equations, or (2) re-form $\underset{\approx}{K}^*$ to include all the new points that have entered V_p and solve this new set of equations. The former method will require more iterations, though the

$\overset{*}{\underset{\approx}{K}}$ matrix will already have been formed and factorised. During this iterative process unloading at certain points may occur; however, experience indicates that this does not present problems and a converged solution is always attained, except in the case where a limit load is approached for perfectly plastic materials. The efficiency of the various schemes is discussed with the numerical examples in Chapter 7.

If large strain increments are allowed the errors produced by these schemes can be substantial. By dividing the excess stress into subincrements, and scaling back the stresses to the yield surface in several stages, this error is reduced. Various subincrementation schemes are in existence. Schreyer, Kulak and Kramer (1979) suggest the following scheme: first, the possible error may be estimated by comparing the angle between the beginning-of-step unit normal and the trial state unit normal, i.e.

$$\theta_e = \cos^{-1}\left(\frac{\underset{\sim}{s}_o \overset{n}{\underset{\approx}{}} \underset{\sim}{s}_t}{s_o \, s_t}\right)$$

where $\underset{\sim}{s}_o$ and s_o are the deviatoric and invariant stresses on the initial yield surface, respectively, and $\underset{\sim}{s}_t$ and s_t are the corresponding values for the trial state. The number of subincrements is then given by

$$N = 1 + \frac{\theta_e}{k}$$

where N is the next lowest integer and k a positive number chosen on the basis of numerical experience.

A simpler formula is given by Hinton and Owen (1980) where the number of subincrements, N, is the nearest integer which is less than

$$\left[\frac{s_t - s_o}{s_y}\right] 8 + 1$$

where s_t and s_o are the trial state and beginning-of-step effective stresses, respectively, and s_y is the initial yield stress, before any work-hardening has taken place and is usually related to the uniaxial yield stress.

The latter measure is implemented in the computer program written for this thesis.

6.5 Program Description

The computer program to analyse elastic-plastic plates was written in ASCII-FORTRAN level 9R1 and implemented on a UNIVAC 1100. A detailed program description, user's manual and program listing is available under separate cover. On the following page we present a macro-flowchart to clarify the salient features of the program.

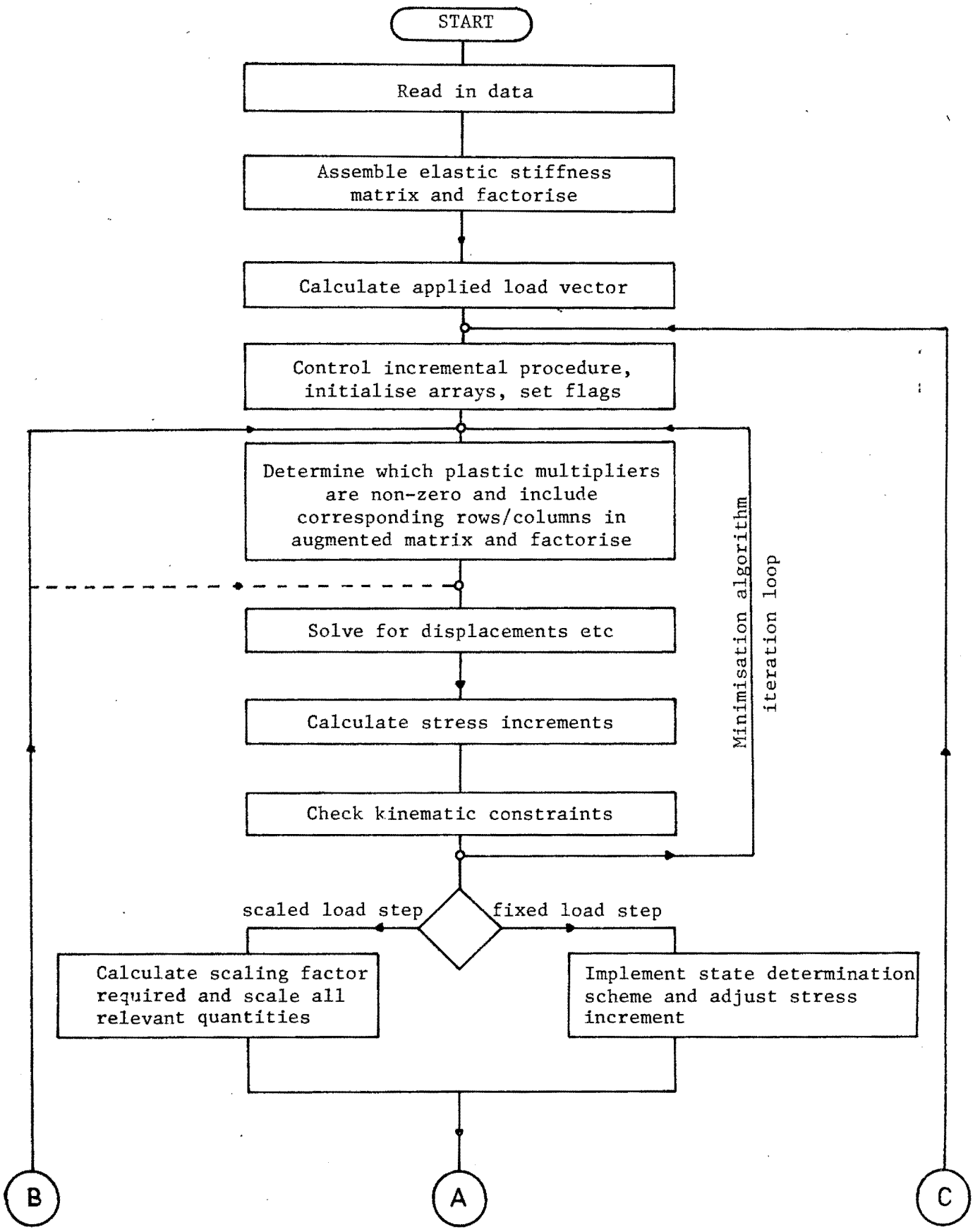
START
Read in data
Assemble elastic stiffness matrix and factorise
Calculate applied load vector
Control incremental procedure, initialise arrays, set flags
Determine which plastic multipliers are non-zero and include corresponding rows/columns in augmented matrix and factorise
Solve for displacements etc
Calculate stress increments
Check kinematic constraints
Minimisation algorithm iteration loop
scaled load step
fixed load step
Calculate scaling factor required and scale all relevant quantities
Implement state determination scheme and adjust stress increment
B
A
C

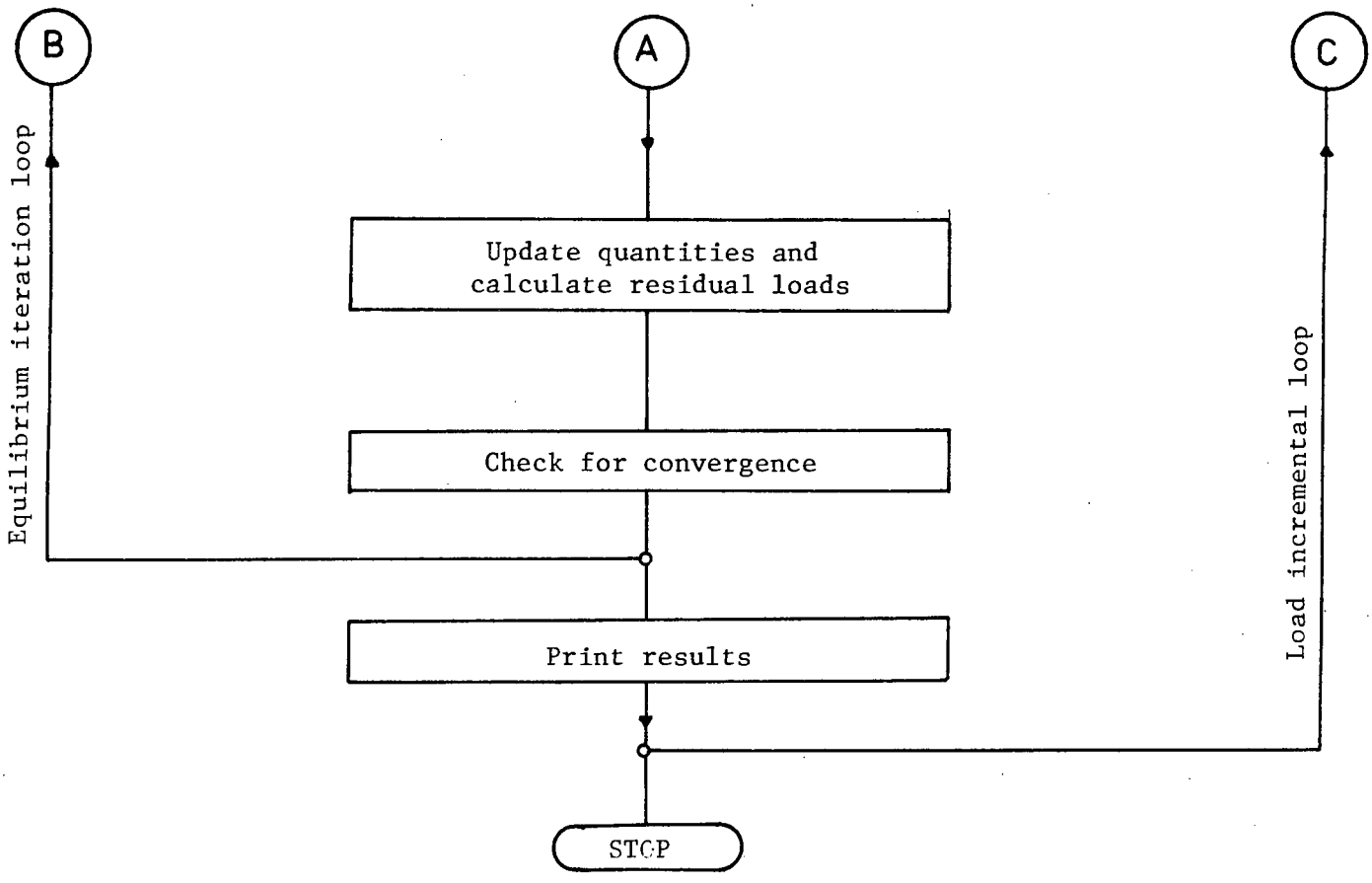

Note: If the augmented stiffness matrix is reformed at the beginning of the load step only the equilibrium iteration proceeds along dashed line.

CHAPTER 7

NUMERICAL EXAMPLES

7.1 Introduction

To illustrate the application of the extended minimum principle using the finite element method to plate bending problems we present selected results which are compared with closed-form solutions (where they exist) and with results using the programs of others. First a limit analysis of a circular plate with simply supported and clamped edges loaded with a uniformly distributed load and a point point is given. Next a similar analysis for a square plate is discussed. The results for a cyclic loading programme for a circular plate with hardening are also presented. Finally, a circular plate with a central hole and a cruciform plate are analysed.

7.2 Circular Plate

The limit load for a simply supported circular plate subjected to a uniformly distributed load assuming a Tresca yield condition can be found analytically, due to the simplicity of the governing equations and the form of the yield surface. However, for a von Mises yield surface the resulting equilibrium equation is non-linear and it must be integrated numerically. In their book on plastic analysis and design Massonnet and Save (1972) formulate the problem for the Tresca yield condition and give limit loads for the uniformly loaded case and for a point load at the centre. Hopkins and Wang (1954) give the limit

loads for various circular plates using a von Mises yield surface.

To give some measure of the efficiency and accuracy of the present approach a limit analysis was carried out on a simply supported circular plate subjected to a uniformly distributed load. The geometrical description of the plate and the finite element mesh together with the material properties are given in Fig. 7.1. Due to two way symmetry only one quadrant has to be discretised. Comparison is made with the results obtained using the finite element programs ADINA (Bathe (1978)), MINDLIN and MINDLAY (Hinton and Owen (1980)) and the solution given by Hopkins and Wang.

The three finite element programs used for comparison all employ the tangent modulus approach. The ADINA shell element was used as a flat plate. This element has six degrees of freedom at each node, which will result in a slightly larger system stiffness matrix than for a plate bending element. All in-plane displacements along the boundaries were constrained. A modified Newton-Raphson procedure with acceleration or the BFGS update incremental procedure were used. Both MINDLIN and MINDLAY use the heterosis plate bending element; the former is a non-layered formulation in which a section of the plate is assumed to go plastic instantaneously. Hence the yield function may be written in terms of stress resultants only. MINDLAY uses a layered approach, where the plate section is divided into discrete layers and the average stress found for a particular layer. When the stresses in a layer satisfy the yield condition, the layer is assumed to become plastic. For this comparison study the plate was divided into four layers. A full Newton-Raphson incremental procedure was used in these two programs.

Four different solution procedures using the computer program written for this thesis were done. We distinguish each as follows: PLATEØ, PLATE1, PLATE2, PLATE3. PLATEØ is the 'exact' solution to the extended kinematic minimum principle in which the load step is adjusted as each gauss point goes plastic. The remainder of the solution procedures employ the state determination schemes discussed in Chapter 5. PLATE1 uses the elastic predictor - radial corrector method and PLATE2 the tangent predictor - radial return method. Both these reformulate $\overset{*}{\underset{\approx}{K}}$ only at the beginning of each incremental step. The procedure in which $\overset{*}{\underset{\approx}{K}}$ is reformulated at every iteration is indicated by PLATE3. This is implemented using the tangent predictor - radial return state determination scheme.

All computer runs were done on the UNIVAC 1100 of the University of Cape Town Computer Centre. Plots of load versus central deflection for the three element mesh are shown in Fig. 7.2. Where curves or plot points overlap we show only PLATEØ or PLATE1 solutions, respectively. As all runs were load controlled, to obtain an estimate of the limit load we use the value of the load at the step before the actual limit load is reached. The CPU times and estimated limit loads are given in Table 7.1. The limit loads are expressed as a fraction of the total applied load. From the table we see that all four solutions from the present study over estimate the limit load by about 7%. However, there is a considerable difference in CPU times. Using the PLATE3 scheme one can use less steps for similar accuracy and achieve a halving in CPU time.

A similar set of runs was done for the plate with edges

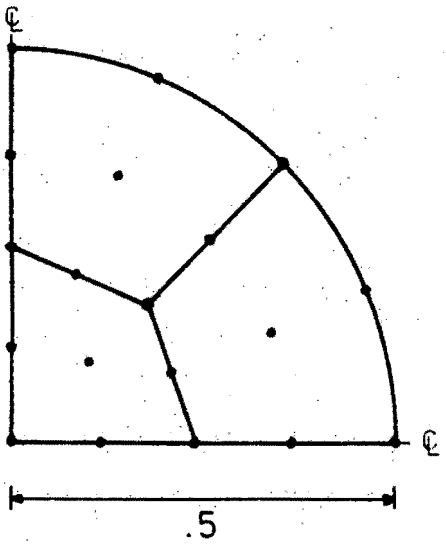

(a) Three Element Mesh

$E = 75.0$ GPa

$\nu = 0.3$

$t = .01$

$\sigma_o = 110.0$ MPa

$M_o = 2.75$ kN

$(M_o = \sigma_o t^2/4)$

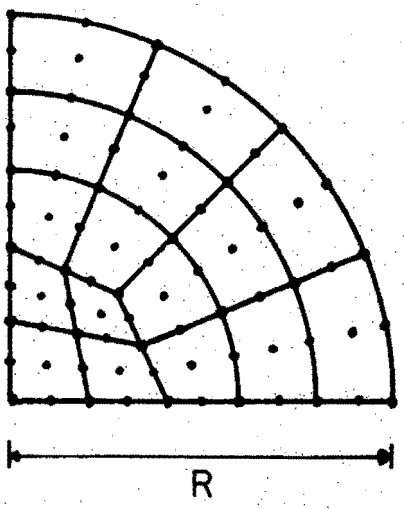

(b) Sixteen Element Mesh

Fig. 7.1 Circular Plate.

Solution	Incremental steps	CPU time (min:sec)	Limit Load
PLATEØ	28	37.57	1.082
PLATE1	7	29.71	1.082
PLATE2	7	29.10	1.082
PLATE3	4	14.25	1.082
ADINA	10	3 : 34.35	1.062
MINDLIN	6	34.81	.895
MINDLAY	15	1 : 38.44	.999

Limit load normalised with respect to Hopkins and Wang : $p = 6.51\ M_o/R^2$

TABLE 7.1 Simply Supported Circular Plate - Uniform Load

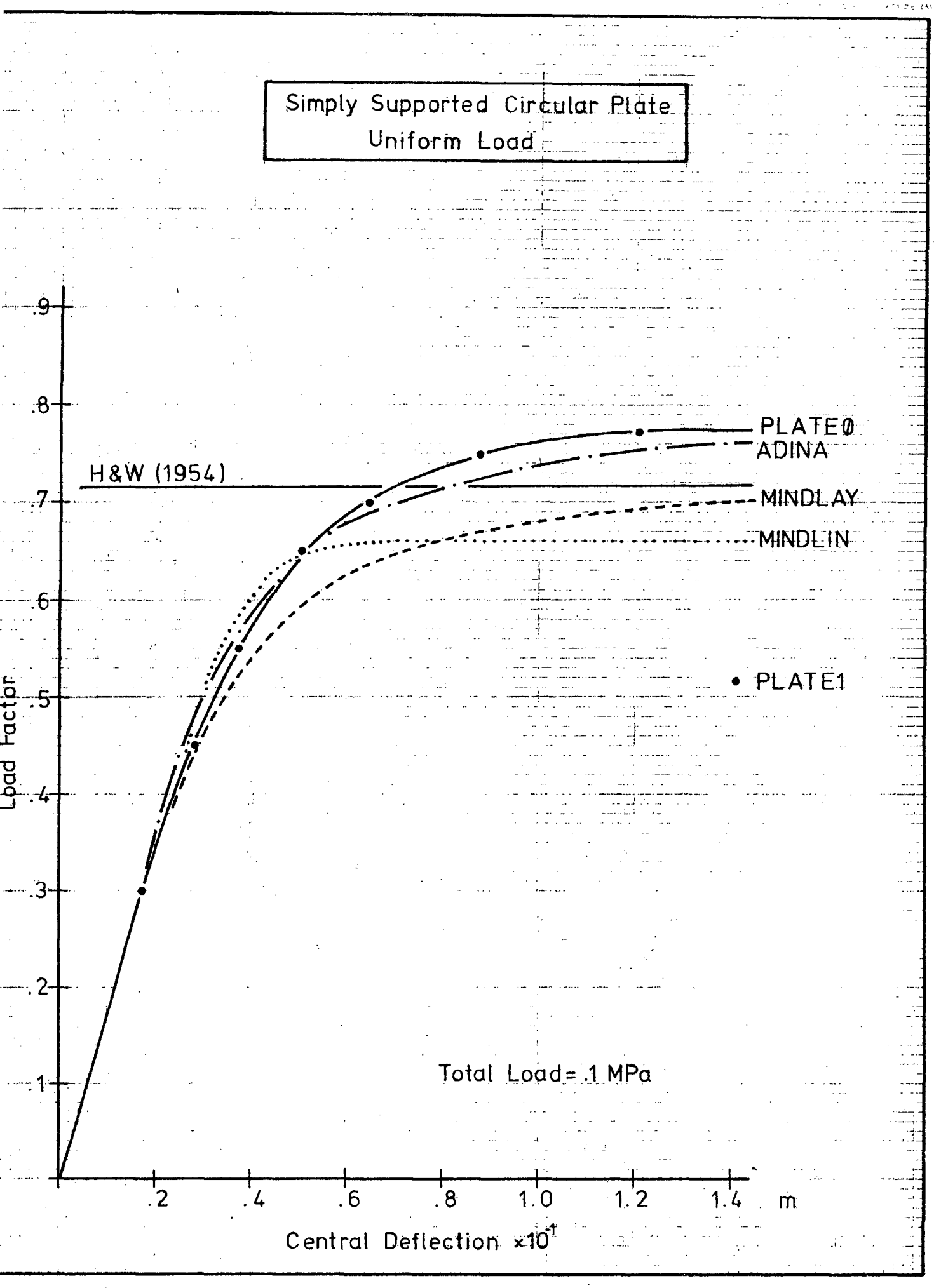
Simply Supported Circular Plate
Uniform Load
Load Factor
.9
.8
.7
.6
.5
.4
.3
.2
.1
H&W (1954)
PLATE0
ADINA
MINDLAY
MINDLIN
PLATE1
Total Load= .1 MPa
.2
.4
.6
.8
1.0
1.2
1.4
m
Central Deflection ×10⁻¹

Fig. 7.2

Solution	Incremental steps	CPU time (min : sec)	Limit Load
PLATE Ø	28	36.48	1.273
PLATE 1	9	21.83	1.273
PLATE 2	9	22.14	1.273
PLATE 3	4	15.41	1.273
PLATE 3*	10	6 : 15.65	1.164
ADINA	6	1 : 39.43	1.455
MINDLIN	8	49.64	1.186
MINDLAY	8	57.41	1.186
Limit load normalised with respect to Hopkins and Wang : $p = 12.5\ M_o/R^2$			

* 16 element mesh

Table 7.2 Clamped Circular Plate - Uniform Load

Solution	Incremental steps	CPU time (min : sec)	Limit Load
PLATE 3	4	17.82	1.297
PLATE 3*	9	12 : 11.74	1.059
ADINA	10	3 : 08.78	1.389
ADINA*	14	22 : 25.84	1.111
Limit load normalised with respect of Hopkins and Wang : $P = 2\pi\ M_o$			

* 16 element mesh

Table 7.3 Simply Supported Circular Plate - Point Load

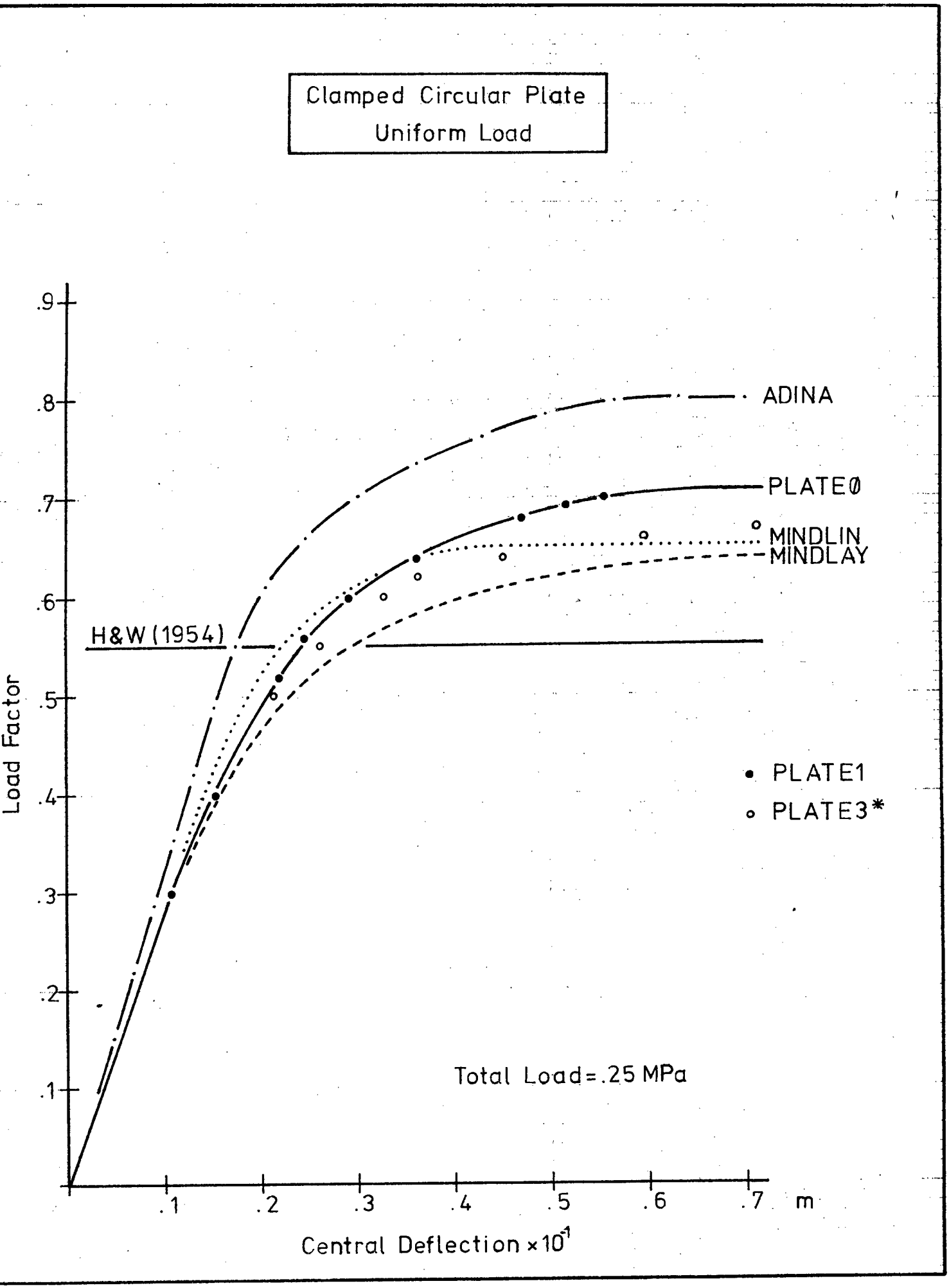
Clamped Circular Plate
Uniform Load
Load Factor
.9
.8
.7
.6
.5
.4
.3
.2
.1
ADINA
PLATE0
MINDLIN
MINDLAY
H&W (1954)
PLATE1
PLATE3*
Total Load=.25 MPa
.1
.2
.3
.4
.5
.6
.7
m
Central Deflection ×10⁻¹

Fig. 7.3

fully clamped. The results are given in Fig. 7.3 and Table 7.2. In this case the estimated limit loads are more than 25% in error. Using a more refined mesh with sixteen elements the difference is still about 15%. However, as can be seen, the CPU time increases significantly. It would seem that to obtain improved results a more refined mesh should be used in the vicinity of the boundary with fewer elements in the centre portion of the plate.

If a point load is applied at the centre of a simply supported plate the results obtained for a three element mesh are approximately 30% more than the limit load given by Hopkins and Wang. The sixteen element mesh reduces this difference to 6%. The results can be misleading as the analytical solution to the limit load neglects the effect of shear forces, which can be quite significant for the concentrated load case. However, we note that shear terms were not included in the yield function used in this study. In Table 7.3 we summarise the above results together with those obtained from ADINA.

7.3 Square Plate

The only available analytical solution for the limit loads of rectangular plates is for a square plate fully clamped subjected to a concentrated load at the centre. Limit analyses of most other plates are confined to the determination of upper and lower bounds for each particular case. These bounds can often differ by as much as 50%. Hodge and Belytschko (1968) formulate the bounds for limit loads as mathematical programming problems. They use finite element techniques to represent velocity and moment fields for the upper and lower bound problems, respectively. The results they obtained are compared to the

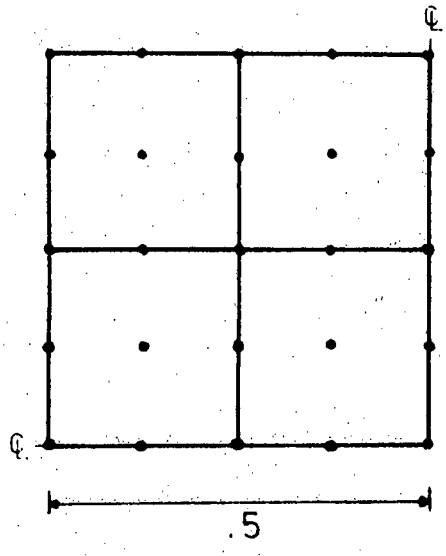

(a) Four Element Mesh

$E = 75$ GPa

$\nu = 0.3$

$t = 0.01$

$\sigma_o = 110$ MPa

$M_o = 2.75$ kN

$(M_o = \sigma_o t^2/4)$

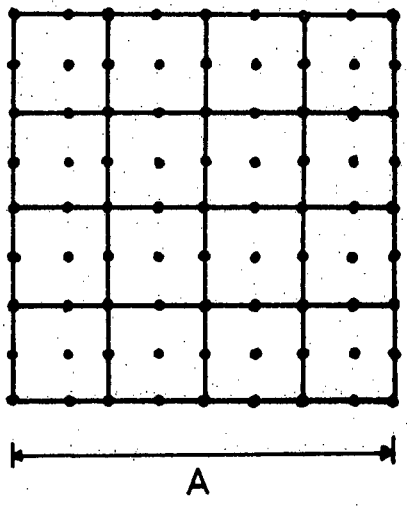

(b) Sixteen Element Mesh

Fig. 7.4 Square Plate.

Solution	Incremental steps	CPU time (min : sec)	α
PLATEØ	37	1 : 01.31	1.136
PLATE1	9	29.00	1.136
PLATE2	9	29.06	1.136
PLATE3	4	17.64	1.136
ADINA	8	1 : 50.87	1.242
MINDLIN	9	56.03	.994
MINDLAY	8	1 : 20.99	1.045
H∝B(1968)	$\alpha = \frac{pA^2}{6M_o}$		1.106
Hodge(1959)			1.155

TABLE 7.4 Simply Supported Square Plate, Uniform Load.

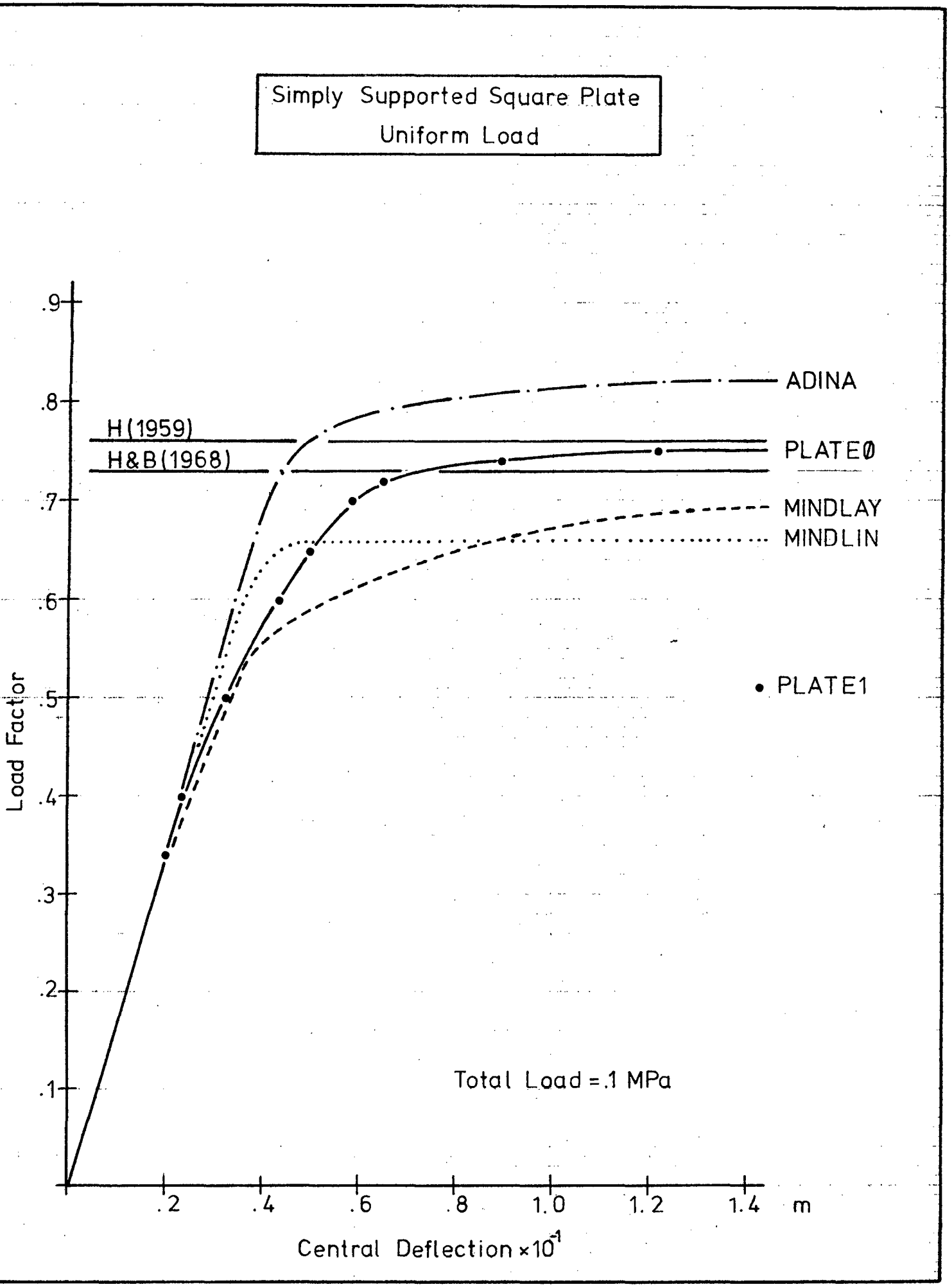
Simply Supported Square Plate
Uniform Load
.9
.8
.7
.6
.5
.4
.3
.2
.1
Load Factor
H(1959)
H&B(1968)
ADINA
PLATEØ
MINDLAY
MINDLIN
PLATE1
Total Load = .1 MPa
.2
.4
.6
.8
1.0
1.2
1.4
m
Central Deflection ×10⁻¹

Fig. 7.5

Solution	Incremental steps	CPU time (min : sec)	α
PLATE Ø	40	1 : 08.92	2.394
PLATE 1	9	25.66	2.394
PLATE 2	9	25.98	2.394
PLATE 3	4	17.34	2.394
PLATE 3*	7	4 : 58.09	2.197
ADINA	7	1 : 16.42	3.106
MINDLIN	4	34.97	2.121
MINDLAY	6	57.38	2.121
H&B(1968)	$\alpha = \frac{pA^2}{6M_o}$		2.052
S&J(1963)			2.310

* 16 element mesh

Fig. 7.5 Clamped Square Plate, Uniform Load

Solution	Incremental steps	CPU time (min:sec)	Limit Load (mp_a)
PLATE 3	7	1 : 49.22	.070
ADINA	14	5 : 15.10	.068

Fig. 7.6 Simply Supported Circular Plate with Central Hole

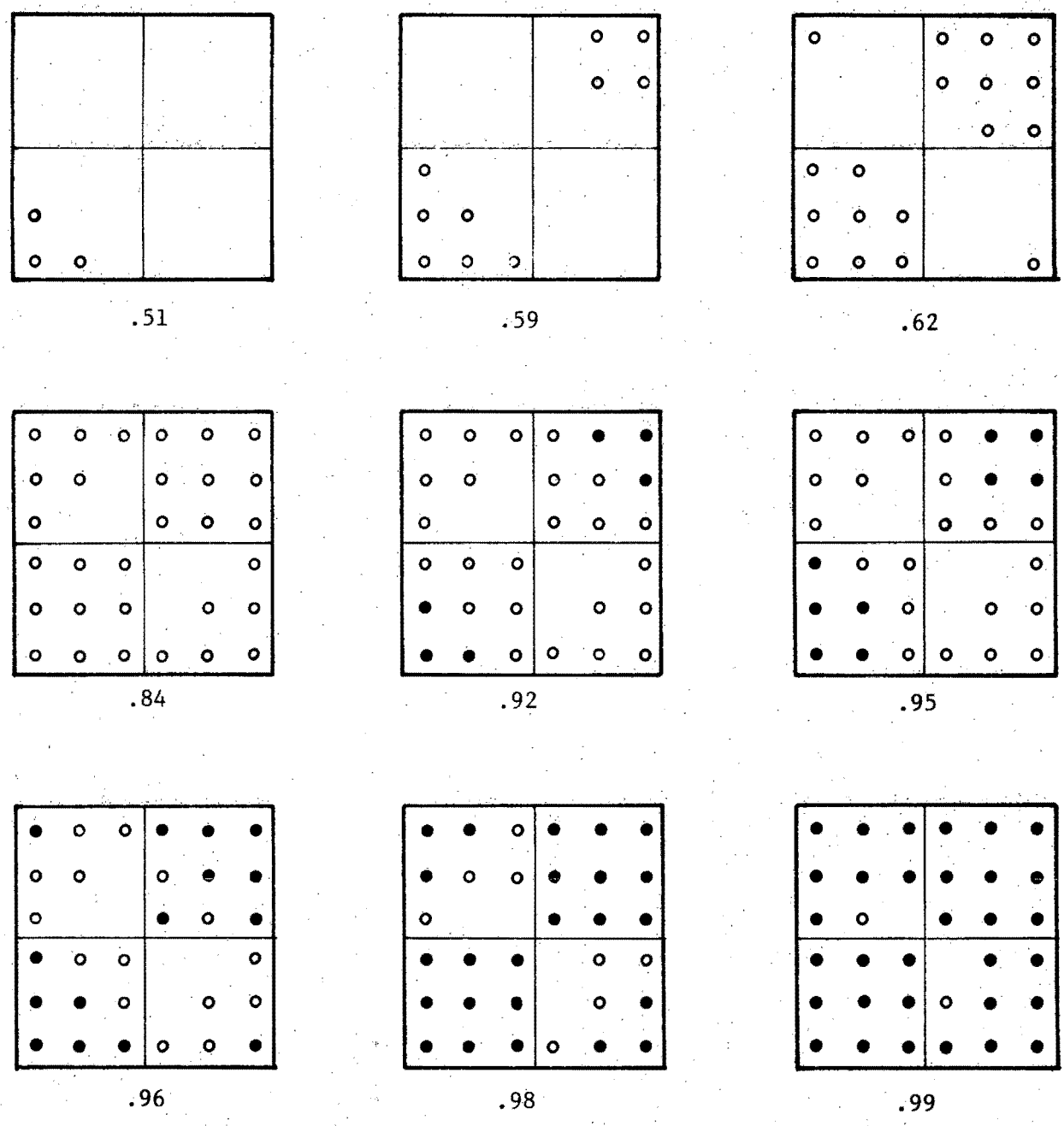

Fig. 7.7 Plastification of Simply Supported Squate Plate
(Numbers indicate fractions of the limit load).

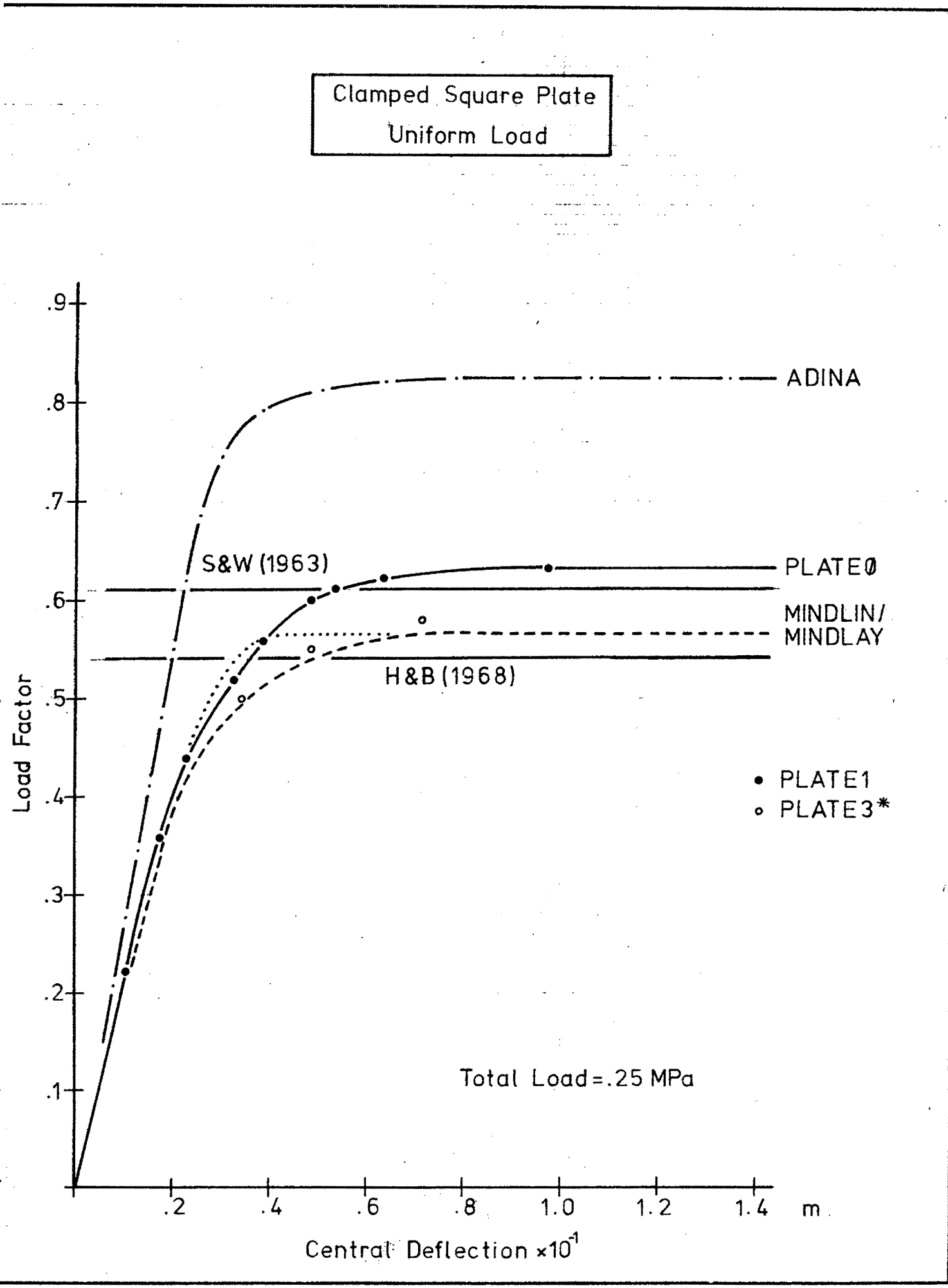
Clamped Square Plate
Uniform Load
.9
.8
.7
.6
.5
.4
.3
.2
.1
Load Factor
ADINA
S&W (1963)
PLATE∅
MINDLIN/
MINDLAY
H&B (1968)
• PLATE1
∘ PLATE3*
Total Load=.25 MPa
.2
.4
.6
.8
1.0
1.2
1.4
m
Central Deflection ×10⁻¹

Fig. 7.8

bounds determined by Hodge (1959) and Sawezuk and Jaeger (1963).

A similar analysis procedure as for the simply supported circular plate was carried out for a simply supported square plate loaded uniformly. The geometrical description with material properties is shown in Fig. 7.4. Again due to two-way symmetry only one quadrant is discretised. Rotations along the boundary were restrained and the corners of the plate prevented from lifting. Curves of load versus central deflection are given for the various computer programs in Fig. 7.5. A summary of computer times and estimated limit loads is given in Table 7.4. As may be seen the results for all programs are in close agreement with the upper bounds given by Hodge and Belytschko. However, as for the circular plate the CPU time for PLATE3 is significantly less. In Fig. 7.7 we give a schematic representation of the development of plasticity across and through the plate. Stresses are calculated at the gauss points. A circle indicates that the surface gauss point has gone plastic and a solid dot indicates that the two interior gauss points are plastic.

The results obtained for the edges of the plate fully restrained are given in Fig. 7.8 and Table 7.5. Limit loads for the four element mesh differ substantially from the upper bound given by Hodge and Belytschko. Using a sixteen element mesh however the difference reduces to 7%. We note that this mesh gives a limit load 4% below the upper bound as determined by Sawzuk and Jaeger.

7.4 Cyclic Loading

The simply supported circular plate of section 7.2 with a

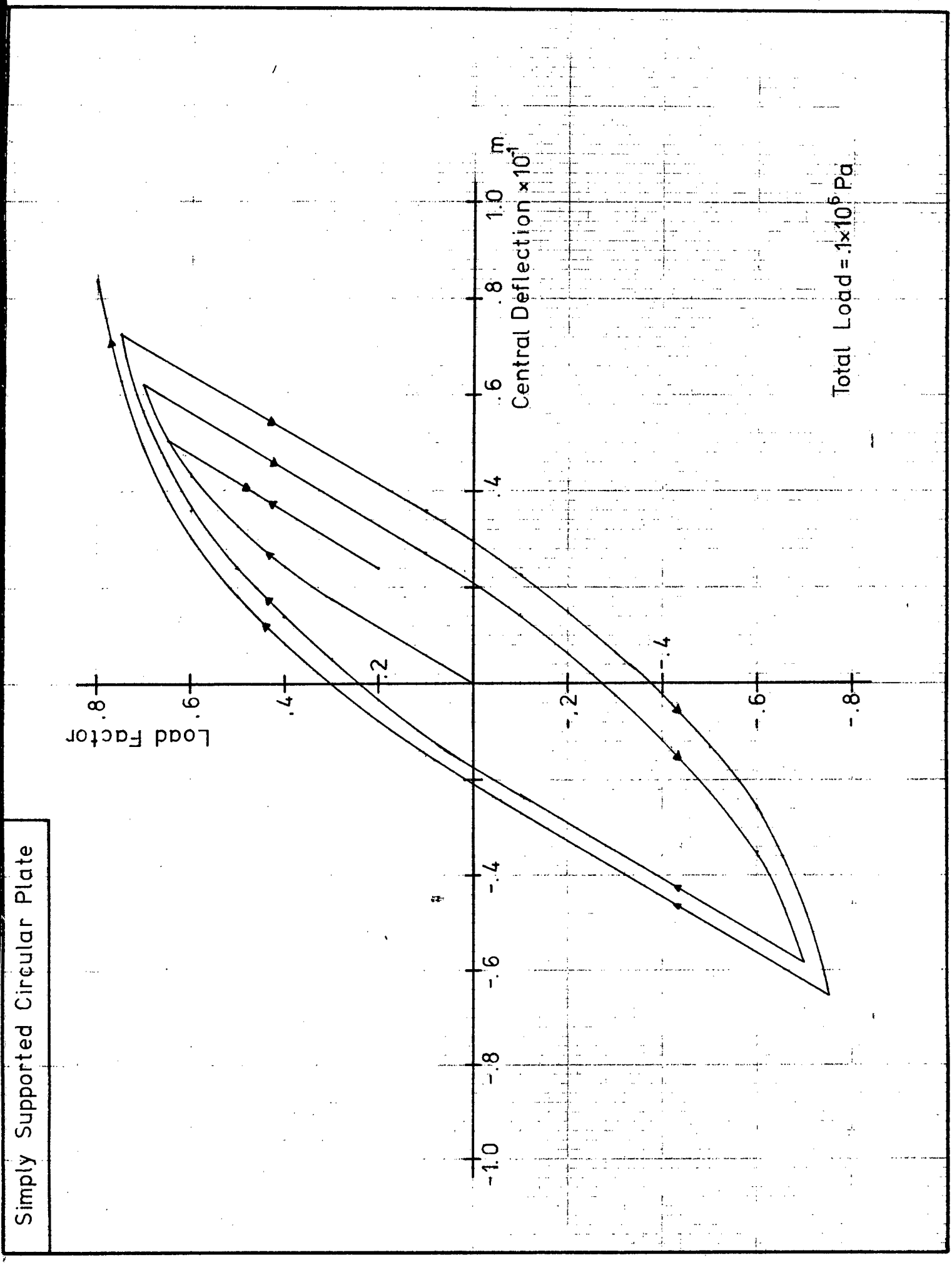

Fig. 7.9 Cyclic Loading Program

uniform load applied was subjected to a cyclic loading programme. The material properties are the same except for that on hardening parameter, c = .2E7, was included.

The plot of load versus central deflection is given in Fig. 7.9. The load is increased monotonically to a load factor of .65 and then decreased to .2 in one step and loaded up to .65 again. Elastic unloading of all the plastic gauss points occurred during the unloading phase and only two iterations of the minimisation algorithm described in section 4.4 was needed to accommodate this. The load factor was then increased to .75 . At this point two complete cycles of the load were applied, each time increasing the highest load factor by .05 . The effect of the isotropic hardening can clearly be seen. Due to the cyclic nature of the load and the multiaxial stress state one or more gauss points may unload during a load increment even though the structure as a whole is loading. The minimisation algorithm accommodated this phenomenum within one iteration each time.

7.5 Circular Plate with Central Hole

In Fig. 7.12 we present a plot of load versus deflection at the inner radius of a simply supported circular plate with its central portion cut out. The geometry and finite element mesh is given in Fig. 7.10 . The plate is assumed to be elastic, perfectly plastic. A comparison between the limit load estimated using the PLATE3 solution procedure and the limit load obtained from Markowitz and Hu (1964) shows a difference of 15%. However, this solution was obtained using a Tresca yield condition. A similar result for the von Mises yield criteria is not available, but it seems reasonable to suggest that the

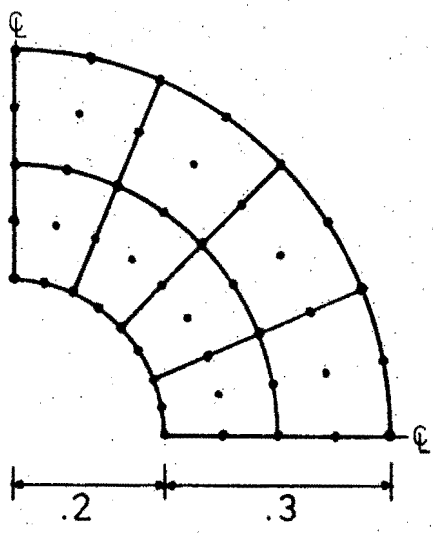

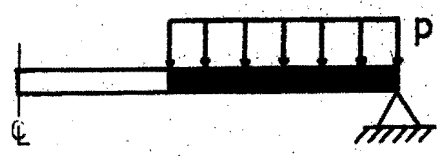

E = 75 GPa

ν = 0.3

t = .01

σ_o = 110 MPa

Fig. 7.10 Circular Plate with Central Hole.

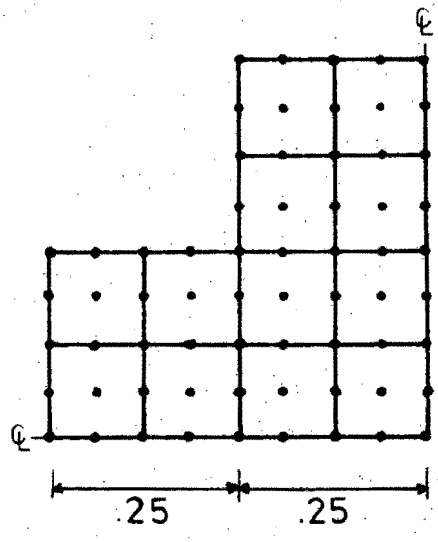

E = 75 GPa

ν = 0.3

t = .01

σ_o = 110 MPa

Fig. 7.11 Cruciform Plate - Simply Supported.

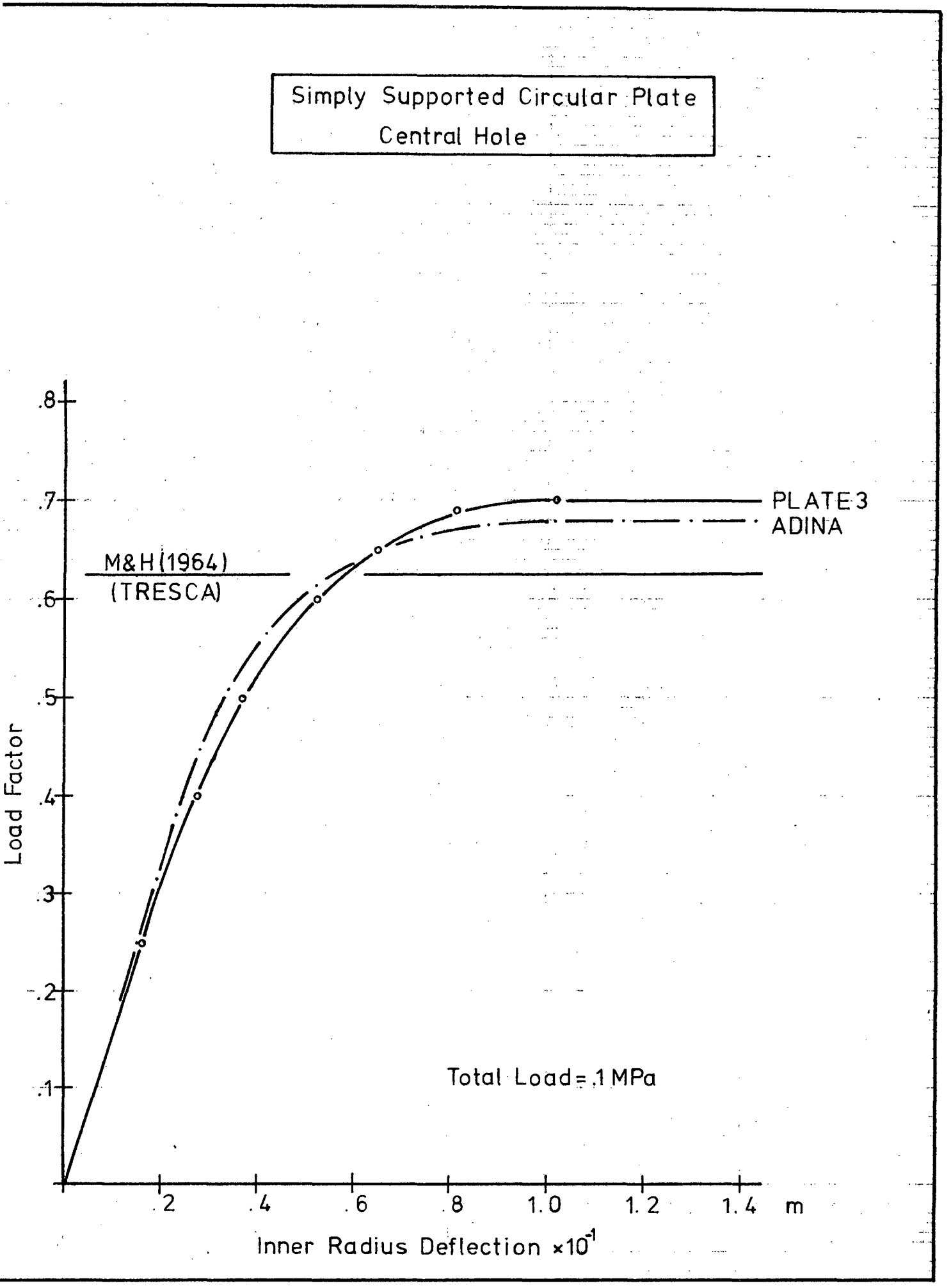
Simply Supported Circular Plate
Central Hole
.8
.7
.6
.5
.4
.3
.2
.1
Load Factor
PLATE 3
ADINA
M&H (1964)
(TRESCA)
Total Load = .1 MPa
.2
.4
.6
.8
1.0
1.2
1.4
m
Inner Radius Deflection ×10⁻¹

Fig. 7.12

numerical result would be substantially closer to the limit load obtained in this manner since for a similar yield value the Tresca yield surface inscribes that of von Mises. In Table 7.6 we give the above results together with those obtained using the ADINA program.

7.6 Cruciform Plate

As a final example we give a schematic representation of the gradual plastification for a simply supported cruciform plate, Fig. 7.11, with a uniform load applied. The plastic state of the plate at six different load factors is shown in Fig. 7.13. Note that the stress concentration around the elbow causes this region to be plastic at a considerable lower load than for the rest of the structure. The effective stress for the gauss point closest to the corner is almost an order of magnitude more than the stress at the gauss points further away in the mesh. For a more accurate result it is obvious that a refinement of the mesh around the point would be needed.

We conclude by noting that experimental load-deflection curves for metal plates differs from that obtained from a limit analysis for pure bending behaviour as one approaches the limit load. This is due mainly to the fact that at the deflections, membrane effects start to dominate and the plates tend to stiffen. However, the failure criterion applied to plates is often not the load capacity, but a prescribed deflection.

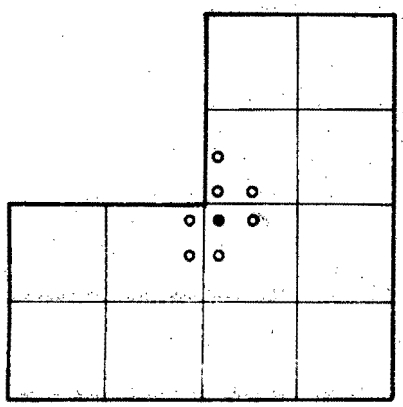

.43

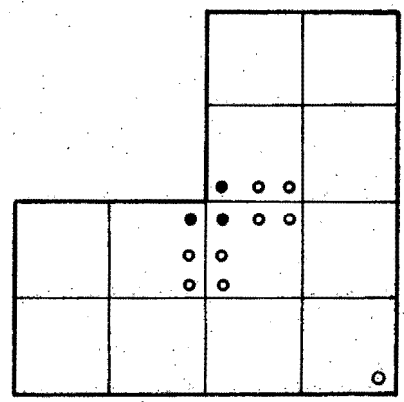

.57

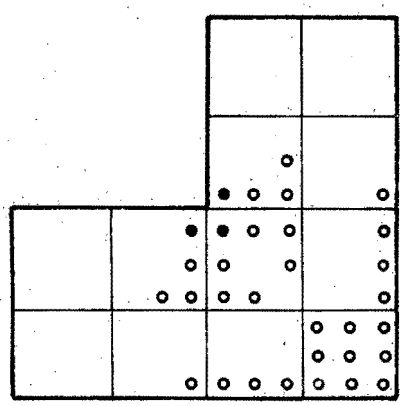

.65

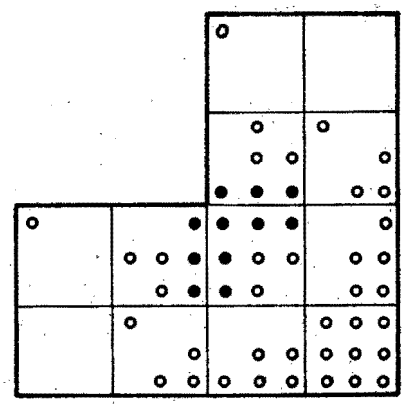

.74

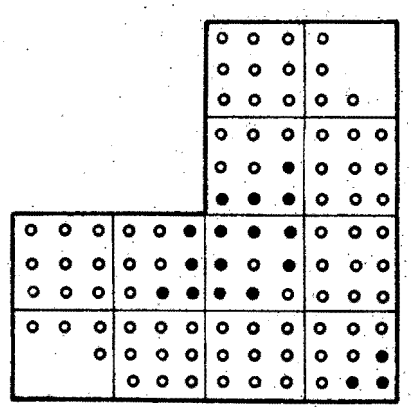

.91

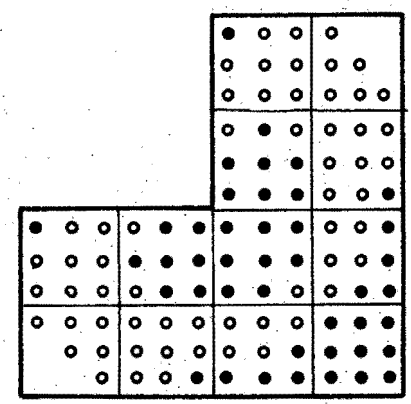

.99

Fig. 7.13 Plastification of Simply Supported Cruciform Plate (Numbers indicate fractions of the limit load).

CHAPTER 8

CONCLUSIONS

In this study we have taken the extended minimum principle of Martin (1975) and have applied it to plate bending problems. For the numerical solution of the minimum principle we have used the finite element method, in particular the heterosis plate bending element of Hughes and Cohen (1978), in conjunction with a simple minimisation algorithm. In addition we have been able to make the solution more efficient by utilising the elastic-plastic state determination schemes to estimate plastic strains not accounted for in the augmented stiffness matrix.

In numerical tests the present approach compares favourably with the available analytical solutions or upper bounds, and with results obtained from other numerical procedures based on the tangent modulus approach. The level of efficiency of the computer program written for this thesis measured on the basis of CPU time, has been shown to be high for the problems presented. However, for a large finite element mesh containing a large number of gauss points in the plastic range the CPU times increase due to the considerable increase in size of the stiffness matrix, which in turn also necessitates a large amount of core storage. However, by the use of a blocked out-of-core solver the program size can still be kept to within reasonable limits. Although the elastic stiffness matrix has to be inverted once only, the amount of effort required to invert the additional rows and

columns due to the plasticity of the body will soon approach that of the effort required to invert the system matrix in the tangent modulus approach. For excessively large meshes the size of the augmented stiffness matrix will obviously be too large for a reasonable solution. However, for the problems presented the present approach usually requires fewer incremental steps to reach the limit load when compared to the tangent modulus approach.

The solution procedure PLATEØ, in which the load step is scaled according as the gauss points become plastic, may be used to determine the elastic range of a loaded body and the point of first yield. In addition, a very good approximation to the limit load can be obtained with only one computer run. For the conventional fixed load step incremental procedure, some trial and error is usually necessary before an estimate of the limit load can be obtained.

It can thus be seen that the method presented in this thesis, is ideally suited to certain applications, for example in limit analyses where the plastic region at collapse is not too great or for large problems in which the plastic region is small compared to the rest of the mesh (e.g. problems involving stress concentrations).

REFERENCES

ANG, A.H. and LOPEZ, L.A. (1968). Discrete Model Analysis of Elastic-Plastic Plates, J. Eng. Mech., ASCE, EM1, 271.

BARLOW, J. (1976). Optimal Stress Locations in Finite Element Models, Int. J. Num. Meth. Engng. Vol.10, 243.

BARNARD, A.J. and SHARMAN, P.W. (1976). The Elastic-Plastic Analysis of Plates using Hybrid Finite Elements, Int. J. Num. Meth. Engng. Vol.10, 1343.

BATHE, K.J. (1978). ADINA - A Finite Element Program for Automatic Incremental Nonlinear Analysis, REP. 82448 - 1, MIT.

BATHE, K.J. and BOLOURCHI, S. (1980). A Geometric and Material Non-linear Plate and Shell Element, Comput. Structures, Vol.11, 23.

COTTLE, R.W. (1977). Fundamentals of Quadratic Programming and Linear Complementarity, Engineering Plasticity by Mathematical Programming, Proc. NATO Advanced Study Inst., University of Waterloo, (Pergamon Press).

DEDONATO, O. and FRANCHI, A. (1977). Elastic-plastic Analysis by Finite Elements, Engineering Plasticity by Mathematical Programming, Proc. NATO Advanced Study Inst., University of Waterloo, (Pergamon Press).

DITTMER, C. (1978). A Programming Approach to the Numerical Solution of Elastic-Plastic Continua, Ph.D Thesis, University of Cape Town.

GALLAGHER, R.H. (1969). Analysis of Plate and Shell Structures, Proc. Sym. Application of Finite Element Methods in Civil Engineering, ASCE, Van Der Bilt University.

GREENBERG, H.J. (1949). Complementary Minimum Principles for an Elasto-plastic Material, Quart. Appl. Math., Vol.7, 85.

HODGE, P.G. and BELYTSCHKO, T. (1968). Numerical Methods for the Limit Analysis of Plates, J. Appl. Mech., ASME, 796.

HODGE, P.G. (1959). Plastic Analysis of Structures, (McGraw-Hill, N.Y.).

HODGE, P.G. and PRAGER, W. (1948). A Variational Principle for Plastic Materials with Strain Hardening, J. Math. & Phys. Vol.27, 1.

HOPKINS, H.G. and WANG, I.J. (1954). Load-carrying Capacities for Circular Plates at Perfectly-plastic Material with Arbitary Yield Condition, J. Mech. Phys. Solids, Vol.3, 117.

HUGHES, T.J.R., TAYLOR, R.L. and KANOKNUKULCHAI, W. (1977). A Simple and Efficient Finite Element for Plate Bending, Int. J. Num. Meth. Engng. Vol.11, 1529.

HUGHES, T.J.R. and COHEN, M. (1978). The 'Heterosis' Finite Element for Plate Bending, Comput. Structures, Vol.9, 445.

HUGHES, T.J.R., COHEN, M. and HARROUN, M. (1978). Reduced and Selective Integration Techniques in the Finite Element Analysis of Plates, Nuclear Engng. Design, Vol.46, 203.

HUGHES, T.J.R. and TEZDUYAR, T.E. (1981). Finite Elements Based Upon Mindlin Plate Theory with Particular Reference to the Four-node Bilinear Isoparametric Element, J. Appl. Mech. ASME, Vol.48, 587,

IRONS, B.M. (1976). The Semi-Loof Shell Element, Finite Elements for Thin Shells and Curved Membranes, (Wiley) 197.

JAVAHERIAN, H., DOWLING, P.J. and LYONS, L.P.R. (1980). Nonlinear Finite Element Analysis of Shell Structures using the Semi-Loof Element, Comput. Structures, Vol.12, 147.

MAC NEAL, R.H. (1978). A Simple Quadrilateral Shell Element, Comput. Structures, Vol.8, 175.

MAIER, G. (1969). Some Theorems for Plastic Strain Rates and Plastic Strains, J. de Mecanique, Vol.8, 5.

MALKUS, D.S. and HUGHES, T.J.R. (1978). Mixed Finite Element Methods-Reduced and Selective Integration Techniques: A Unification of Concepts, Comput. Meth. Appl. Mech. Engng., Vol.15, 63.

MARCAL, P.V. and KING, I.P. (1967). Elastic-plastic Analysis of Two-dimensional Stress Systems by the Finite Element Method, Int. J. Mech. Sci., Vol.9, 143.

MARKOWITZ, J. and HU, L.W. (1964). Plastic Analysis of Orthotropic Circular Plates, Proc. ASCE, J. Eng. Mech. Div., Vol.90, 251.

MARTIN, J.B. (1975). On the Kinematic Minimum Principle in Classical Plasticity, J. Mech. Phys. Solids, Vol.23, 123.

MARTIN, J.B. (1976). Plasticity: Fundamentals and General Concepts, (MIT).

MARTIN, J.B. and REDDY, B.D. (1977). A Programming Approach to the Solution of the Rate Problem in Elastic, Plastic Solids, Mechanics in Engineering, (University of Waterloo Press).

MARTIN, J.B. (1982). Basic Stress-Strain Relations for Incremental Plasticity, Pre-Conference Sem. on Plasticity FEMSA/82, University of Stellenbosch.

MARTINS, R.A.F. and OWEN, D.R.J. (1981). Elastoplastic and Geometrically Nonlinear Thin Shell Analysis by the Semi-Loof Element, Comput. Structures. Vol.13, 505.

MINDLIN, R.D. (1951). Influence of Rotatory Inertia and Shear on Flexural Motions of Isotropic, Elastic Plates, J. Appl. Mech. Vol.18, 31.

OWEN, D.R.J. and HINTON, E. (1980). Finite Elements in Plasticity: Theory and Practice, (Pineridge).

PARISCH, H. (1979). A Critical Survey of the 9-node Degenerated Shell Element with Special Emphasis on Thin Shell Application and Reduced Integration, Comput. Meth. Appl, Mech. Engng. Vol.20, 323.

POPOV, E.P., KHOJESTEH-BAKHT, M. and YAGHMAI, S. (1967). Analysis of Elastic-Plastic Circular Plates, J. Eng. Mech., ASCE, EM6, 49.

PUGH, E.D.L., HINTON, E. and ZIENKIEWICZ, O.C. (1978). A Study of Quadrilaterial Plate Bending Elements with Reduced Integration, Int. J. Num. Meth. Engng., Vol.12, 1059.

ROBINSON, J. (1979). LORA - An Accurate Four Node Stress Plate Bending Element, Int. J. Num. Meth. Engng., Vol.14, 296.

SAVE, M.A. and MASSONET, C.E. (1972). Plastic Analysis and Design of Plates, Shells and Disks, (North-Holland).

SAWCZUK, A. and JAEGER, T. (1963). Grenztragfahigskeit-Theorie der Platten, (Springer-Verlag, Berlin).

SAYEGH, A.F. and RUBINSTEIN, M. (1972). Elastic-plastic Analysis by Quadratic Programming, Proc. Eng. Mech. Div., ASCE, Vol.98, EM6, 1547.

SCHREYER, H.L., KULAK, R.F. and KRAMER, J.M. (1979). Accurate Numerical Solutions for Elastic-Plastic Models, J. Pressure Vessel Tech., ASME, Vol.101, 226.

SPILKER, R.L. and MUNIR, N.I. (1980). A Serendipity Cubic-Displacement Hybrid-Stress Element for Thin and Moderately Thick Plates, Int. J. Num. Meth. Engng., Vol.15, 1261.

WILSON, E.L., BATHE, K.J. and DOHERTY, W.P. (1974). Direct Solution of Large Systems of Linear Equations, Comput. Structures, Vol.4, 363.

ZIENKIEWICZ, O.C., VALLIAPAN, S. and KING. I.P. (1969). Elasto-plastic Solutions of Engineering Problems Initial Stress, Finite Element Approach, Int. J. Num. Meth. Engng., Vol.1, 75.